


11-12-2021

Evaluating Changes in Visible to Short-Wave Infrared Spectral Reflectance of Arctic Mosses in Response to Experimental Drying to Find the Best Predictors of Moisture Content

Steven L. Unger

Florida International University, sunge001@fiu.edu

Follow this and additional works at: <https://digitalcommons.fiu.edu/etd>

 Part of the [Botany Commons](#), [Bryology Commons](#), [Environmental Indicators and Impact Assessment Commons](#), [Environmental Monitoring Commons](#), [Other Earth Sciences Commons](#), and the [Terrestrial and Aquatic Ecology Commons](#)

Recommended Citation

Unger, Steven L., "Evaluating Changes in Visible to Short-Wave Infrared Spectral Reflectance of Arctic Mosses in Response to Experimental Drying to Find the Best Predictors of Moisture Content" (2021). *FIU Electronic Theses and Dissertations*. 4880.
<https://digitalcommons.fiu.edu/etd/4880>

This work is brought to you for free and open access by the University Graduate School at FIU Digital Commons. It has been accepted for inclusion in FIU Electronic Theses and Dissertations by an authorized administrator of FIU Digital Commons. For more information, please contact dcc@fiu.edu.

FLORIDA INTERNATIONAL UNIVERSITY

Miami, Florida

EVALUATING CHANGES IN VISIBLE TO SHORT-WAVE INFRARED SPECTRAL
REFLECTANCE OF ARCTIC MOSSES IN RESPONSE TO EXPERIMENTAL
DRYING TO FIND THE BEST PREDICTORS OF MOISTURE CONTENT

A thesis submitted in partial fulfillment of

the requirements for the degree of

MASTER OF SCIENCE

in

BIOLOGY

by

Steven L. Unger

2021

To: Dean Michael R. Heithaus
College of Arts, Sciences and Education

This thesis, written by Steven L. Unger, and entitled Evaluating Changes in Visible to Short-Wave Infrared Spectral Reflectance of Arctic Mosses in Response to Experimental Drying to Find the Best Predictors of Moisture Content, having been approved in respect to style and intellectual content, is referred to you for judgment.

We have read this thesis and recommend that it be approved.

Daniel Gann, Committee Member

Paulo Olivas, Committee Member

Steven Oberbauer, Major Professor

Date of Defense: November 12, 2021

The thesis of Steven L. Unger is approved.

Dean Michael R. Heithaus
College of Arts, Sciences and Education

Andrés G. Gil
Vice President for Research and Economic Development
and Dean of the University Graduate School

Florida International University, 2021

© Copyright 2021 by Steven L. Unger

All rights reserved.

DEDICATION

I would like to dedicate this master's thesis to my loving family who have supported me and my dreams of studying science from a young age. To my Mother, Father, and brother Richard, your eternal love knows no bounds and I treasure you all immensely. My feelings for you all are tacitly ineffable. You have stood by me through great highs and terrible lows, never judged, and always lent your shoulders and ears. Your love and support have driven me to be the best version of myself and I don't know how I can ever repay you. I would particularly like to dedicate this thesis to my uncle William who passed before I got to spend my first field season in the Arctic, back in 2015. Mono, you pushed me to study what I love and not care about what anyone thought and your passion for birds and wildlife lives on in me. Para mis tíos en Colombia (Kike y Dario), gracias por las conversaciones increíbles de la naturaleza, de química y física y del mundo entero. A mi abuelita amorosa Tita, gracias por enseñar me español y crear me con mi mamá cuando mi papá tuvo que trabajar tarde. To my childhood friend, Turo, we have grown up together and faced tons of obstacles along the way, but we can always count on each other. To my little Clementine, your love drives me and to Bry, thank you for pushing me in ways I have never been pushed before, it made me realize what is important for my future and how dedicated I need to be to get there. Thank you Joe, your guidance and support has been invaluable. To the people who have come into my life for a day, a season, a year, or for life, thank you for impacting me and making me who I am today. The lessons learned will not be forgotten and the changes to my character over time will become engrained.

ACKNOWLEDGMENTS

I owe an immense debt of gratitude to Dr. Sergio Vargas, who was vital to the success of this thesis, from a technical and logistical standpoint. Not only did you make this research possible, by accepting my samples for measurement at UTEP, but also by guiding me through the process of analyzing the data and introducing me to great resources. I am tremendously grateful to Dr. Jeremy May, who I have worked with since 2015, and has become a true friend and mentor. Without you and your guidance, I would not have embarked on this journey. To my advisor Dr. Steve Oberbauer, you took a city boy who always dreamed of what wilderness felt like and gave him an opportunity to live in remote Alaska and experience things he could only dream of. Your demeanor and love of science and exploration captivated me, and I will never forget our time in the field in Alaska, away from the hustle and bustle of university life. Your guidance has honed my skills and will continue to drive me forward. To Dr. Daniel Gann, your help in the analytic approach to my thesis and expertise in remote sensing have been invaluable, thank you for taking the time to drive these concepts home. To Dr. Paulo Olivas, your expertise in plant biology and remote sensing as well as your guidance in finalizing this thesis were vital. I gratefully thank the Toolik Arctic Field Station and especially the Environmental Data Center for logistical support. This material is in part based upon work supported by the National Science Foundation under Grant OPP 1836898.

ABSTRACT OF THE THESIS

EVALUATING CHANGES IN VISIBLE TO SHORT-WAVE INFRARED SPECTRAL REFLECTANCE OF ARCTIC MOSSES IN RESPONSE TO EXPERIMENTAL DRYING TO FIND THE BEST PREDICTORS OF MOISTURE CONTENT

by

Steven L. Unger

Florida International University, 2021

Miami, Florida

Professor Steven Oberbauer, Major Professor

Mosses are a dominant understory component in the Arctic and because of sparse canopy cover, contribute to spectral signals used in remote sensing. Unlike vascular plants, mosses cannot actively regulate moisture content and are highly susceptible to desiccation. Previous research has shown that moss reflectance is sensitive to tissue moisture content. Here, a lab-controlled drying experiment was conducted to identify the best spectral predictors of moisture content of moss as well as distinguishing characteristics of their spectral profile. Significant changes in the entire spectrum were observed in response to desiccation. All moisture indices were able to predict moisture content with a reasonable certainty. Derivative spectra can be used to distinguish between moss and vascular plant spectra (slope/inflection point). Lastly, a pilot experiment showed that moisture content of moss can significantly drive community-level spectra *in situ*. These results demonstrate the need to incorporate mosses (w/moisture effects) into spectrally derived models.

TABLE OF CONTENTS

CHAPTER	PAGE
I. Introduction	1
I.1 –Arctic Vegetation Characteristics.....	1
I.2 – Moisture Content of Non-vascular Plants and Remote Sensing.....	1
I.3 – Remote Sensing Indices.....	2
I.4 – Important Remote Sensing Terminology	4
I.5 – Background and Prior Research	5
Table 1: Moisture-related Reflectance Indices	6
I.6 – Tissue Effects on Spectral Reflectance	7
I.7 –The Red Edge Region.....	7
I.8 – Classification and Derivative Spectroscopy in Remote Sensing.....	9
I.9 – Summary of Background Information and Significance	10
I.10 – Statement of Research Objectives and Hypotheses	11
II. Methods.....	13
II.1 - Site Description and Sample Collection	13
II.2 - Sample Handling and Maintenance	14
II.3 - Instrumentation & Measurements.....	15
II.3a - Moss Drying Experiment	15
II.3b - Vascular Plant Spectra	16
II.3c - Community-level Rehydration Experiment	17
II.4 - Analysis Approach	17
II.4a - Moss Drying Experiment	17
II.4b - Moss and Vascular Plant Spectral Comparisons	19
II.4c - Community-level Wetting Experiment.....	19
III. Results and Discussion	20
III.1 - Spectral Profile at Varying Moisture Contents	20
III.2 - Correlation of Moisture Content to Spectral Reflectance Indices.....	22
Table 2: Summary of Spearman Rank Correlations of Spectral Indices ...	23
III.3 – Nonlinear Modeling of Indices as a Function of Moisture Content	23
Table 3: Summary of Nonlinear Logistic Models	26
Table 4: AIC Summary Chart.....	30
III.4 - Moss and Vascular Plant Spectral Comparisons	31
III.4a - Investigating Derivative Spectra.....	31
III.4b – Investigating Red Edge Parameters	34
III.5 – Evaluation of Potential changes in Moss Spectra in Response to Shipping and Handling	36

III.5a – Spectral Indices Evaluation.....	37
III.5b – Red Edge Parameters	38
III.6 - Community-level Wetting Experiment	39
III. Discussion.....	42
III.1 Spectral Reflectance of Mosses During Drying	42
III.2 – Modeling behavior of spectral indices and moisture content of mosses ...	43
III.3 – Derivative Spectra for Identifying Region for Classification.....	45
III.4 – Rehydration Pilot Study.....	46
V. Conclusion	48
Literature cited	50

TABLE OF FIGURES

CHAPTER	PAGE
III. Results and Discussion	20
III.1 - Spectral Profile at Varying Moisture Contents.....	20
Figure 1: <i>S. capillifolium</i> (RS) spectra divided into moisture brackets.....	20
Figure 2: <i>S. lenense</i> (OS) spectra divided into moisture brackets.	21
Figure 3: Mixed pleurocarpous community (MP) spectra divided into moisture brackets	22
III.3 – Nonlinear Modeling of Indices as a Function of Moisture Content	23
Figure 4: Logistic model predictions on testing dataset for <i>S. capillifolium</i> (red sphagnum) (A) and <i>S lenense</i> (orange sphagnum) (B)	28
Figure 5: Logistic model predictions on testing dataset for mixed pleurocarpous moss (MP) (A) and mixed moss (MM) (B).....	29
III.4 - Moss and Vascular Plant Spectral Comparisons	31
III.4a - Investigating Derivative Spectra.....	31
Figure 6: Average spectral signature by group	31
Figure 7: Average spectral profile of moss and vascular plants w/ 95% confidence intervals	32
Figure 8: Raw spectra (A) and first (B) and second derivative (C) spectra for mixed mosses (MM, blue) and Vascular Plants (Vascular, green).....	33
III.4b – Investigating Red Edge Parameters	34
Figure 9: Boxplot comparing moss and vascular plant RESP	34
Figure 10: Boxplot comparing the red edge shoulder of MP (n=136), RS (n = 151), and OS (n = 141)	35
Figure 11: Boxplot comparing different amounts of high and low moisture-content between the three different communities.....	35

III.5 – Evaluation of Potential changes in Moss Spectra in Response to Shipping and Handling.....	36
III.5a – Spectral Indices Evaluation.....	37
Figure 12: WBI boxplot comparison of pre and post shipment. (12b – bottom row) NDVI boxplot comparison of pre and post shipment.....	37
III.5b – Red Edge Parameters	37
Figure 13: Boxplot comparing the pre-shipment moss (n = 50), post shipment moss and vascular plants (n=68).....	37
III.6 - Community-level Wetting Experiment	39
Figure 14: Community-level, leaf-level (vascular), and moss-level spectral profiles are shown at both field dried conditions and experimentally moistened conditions.	39
Figure 15: Boxplot showing NDVI differences between wet (W) and dry (D) conditions of the three groups (Mix or community, moss, and vascular plants)..	40
Figure 16: Boxplot showing NDWI differences between wet (W) and dry (D) conditions of the three groups (Mix or community, moss, and vascular plants)..	41
Figure 17: Boxplot showing MSI differences between wet (W) and dry (D) conditions of the three groups (Mix or community, moss, and vascular plants)..	42

I. Introduction

I.1 – Arctic Vegetation Characteristics

Mosses present unique challenges for the study of arctic vegetation using remote sensing approaches. As a result of permafrost laden soils, frigid long and dark winters, short, intense summer growing seasons, arctic vegetation is largely treeless and is instead dominated by evergreen and deciduous shrubs, graminoids, bryophytes, lichens, and in some areas bare ground [1]. Vegetation is typically less than a meter tall and forms a sparse canopy of vascular plants with mosses and lichens growing on the surface as understory or in the open [1]. Surface reflectance signals used in remote sensing studies of vegetation in the Arctic are a combination of those from vascular plants, nonvascular plants (bryophytes), and lichens, [2, 3], all of which have different tissue optical properties [4]. Many common moss species found throughout much of the Arctic are known to change spectral reflectance properties in response to short-term environmental stressors, such as drought or heat stress [5-8]. As the Arctic rapidly warms, these environmental stressors are becoming more frequent [9, 10].

I.2 – Moisture Content of Non-vascular Plants and Remote Sensing

Unlike vascular plants, which can absorb water into their tissues via root systems, mosses (poikilohydric bryophytes) cannot actively regulate internal moisture content and are thus more susceptible to moisture fluctuations. However, most mosses are more resilient to tissue damage caused by short-term drought [11, 12]. As a result, mosses may become desiccated well before vascular plants show signs of water stress. Even after

rainfall, under warm windy conditions, mosses can dry out very quickly at the tops of hummocks (S. Unger, personal observation). Some moss species that undergo temporary desiccation exhibit dramatic spectral changes with drying, which can be quantified using spectrometers and derived remotely-sensed spectral indices [13]. Some studies have shown that these changes in reflectance (some apparent as color changes) are also associated with changes in photosynthetic potential [8, 14-16]. Despite the importance of mosses to the structure and function of arctic ecosystems (soil temperature regulation and moisture retention [17]) and their contributions to ecosystem gross primary productivity (GPP)[18], only a few studies have addressed the issue of the potential effects of mosses on remotely-sensed vegetation indices [3, 13, 16]. This aspect is of particular importance because many of these indices have been primarily developed from and for vascular plants [19-22]. We know that moss reflectance changes significantly as a function of moisture content [8, 13, 16], but the question remains: in what way is the spectra changing and to what extent is it driving satellite spectra signals?

I.3 – Remote Sensing Indices

In arctic regions where remoteness and scale of study area are serious limitations to ground-based measurements, remote sensing methods are being rapidly adopted to monitor ecosystem responses to environmental change. Scientists have developed vegetation-derived relationships between absorption and reflectance of biologically significant wavelengths that can be used to estimate vegetation cover and productivity. Spectral relationships (indices), such as the Normalized Difference Vegetation Index (NDVI) and the Photochemical Reflective Index (PRI) can provide details about

phenology, estimates of biomass, and the status of vegetation photosynthetic efficiency, with the ultimate aim of predicting ecosystem GPP [3, 23, 24]. One of the most commonly employed indices is NDVI because of its strong relationship with green biomass, that results from the strong absorbance of red wavelengths and strong reflectance of near infrared (NIR) wavelengths by plant leaves [25]. By correlating these reflectance behaviors with environmental variables, such as temperature and precipitation to form spectral-ecological relationships, NDVI can be used as a proxy to estimate productivity, track phenological events, leaf area index (LAI) to detect vegetation community shifts, monitor drought and water stressed vegetation, and land degradation/rehabilitation [24, 26-35]. However, these relationships rely on ground-based measurements that may inadequately represented for larger regions. Unlike temperate and tropical regions where most of the relationships have been derived, the generally sparse canopies of arctic vegetation are comprised of significant amounts of moss and lichen along with vascular plants [2, 3]. While NDVI has been somewhat supplanted by more robust indices, it is still used ubiquitously, and now comes as a basic product from many satellite imagery products and can be of great value when accounting for its limitations such as saturation at high LAI [36].

I.4 – Important Remote Sensing Terminology

Resolution is used in four ways in remote sensing: spatial, temporal, spectral, and radiometric. Spatial resolution is simply the size of the pixel which is collected [37]. With very high resolution you may have pixels of 2x2m while low resolution may provide more than 300x300m pixels. Temporal resolution refers to the frequency of measurement

at the same location, essentially what the revisitation time of the satellite is (i.e. every 14 days vs daily) [37]. Spectral resolution refers to the number and dimensions of bands or channels that a sensor is sensitive to [37]. With high spectral resolution, the number of bands increases and their width decreases indicating and vice-versa. Radiometric resolution refers to the sensitivity of light intensity perceived by the sensor, thus high radiometric resolution implies ability to distinguish between various levels of brightness, whereas low resolution means that differences in levels of brightness are harder to detect [37].

With advances in sensor technology, hyperspectral reflectance measurements (sensor dividing the spectrum into many continuous spectral bands) have become more widely available. For instance, a multispectral sensor platform such as Landsat 8 has 11 spectral bands (fewer and broader bands) and can be utilized to map a forest, whereas a hyperspectral sensor platform such as AVIRIS-NG has 425 contiguous spectral bands and can be used to map different tree species in that forest. Various tradeoffs exist between Ground-based sensors and satellite or ariel sensor platforms and between the four types of resolution, which ultimately determines which sensor platform a researcher chooses to use based on their scientific objectives. For example, giving up spatial resolution for better temporal resolution may be suited to arctic studies given the condensed growing season (~ 3 months), so more frequent repeat imagery (1-5 days) can provide more meaningful details about ecosystem processes such as phenology compared with higher spatial resolution, but low temporal resolution (16+ day revisitation). My research focuses on ground-based sensors (in the lab and field) with high spectral and

temporal resolution with the hope of eventually scaling up our findings to both multispectral and hyperspectral satellite platforms.

I.5 – Background and Prior Research

A prior experiment conducted by our group demonstrated that moss reflectance metrics, specifically the commonly used spectral index NDVI, changes significantly in response to large short-term moisture fluctuations, which does not necessarily correlate to observed changes in photosynthetic activity [16]. These changes were largely driven by increases of red reflectance [16]. We found a strong correlation between a decrease in moisture content and subsequent decrease in NDVI and photosynthetic function of four dominant arctic moss species that were isolated from vascular plants under controlled conditions. Moreover, subsequent rehydration rapidly restores initial NDVI values (in a matter of minutes), however photosynthetic function takes far longer to recover (several hours to days) [16]. This physiological lag introduces uncertainty when evaluating satellite-derived estimates of productivity. While reflectance may have rebounded quickly, moss photosynthesis did not. Furthermore, if spectrally-driven ecosystem flux models [3, 38] assume that the moss-driven decrease in NDVI reflects decrease in vascular plant biomass, even larger errors would be introduced. The result is that erroneous estimation of GPP or LAI can occur and are dependent on the amount of moss within the pixels and what moisture content they are at when imagery was collected. If community-level spectra are significantly driven by mosses (and their moisture content), then vegetation classes which are not reflected in the look-up tables for the interpretation of NDVI need to be adjusted to incorporate mosses. Thus, to decompose the signal, we

need better understanding of two principles; 1. The effects of moisture content on moss endmember spectra and 2. Features of the moss spectral signature that is unique to mosses for classification purposes.

Our prior study was limited to the VIS-NIR region of the spectrum (350-1,050 nm) by the spectrometer available (Unispec-SC, PP Systems, Haverhill MA). The short-wave infrared region (SWIR: 1,100-2500 nm) is known to be sensitive to water absorption features [13]. Various moisture indices have been developed using both ranges to assess the moisture content of vegetation and soils based on the attenuation of light by water molecules (Table 1).

Table 1. Moisture-related reflectance indices

Spectral Reflectance Index	Abr	Formula	Ref
Water Band Index	WBI	R_{900}/R_{970}	[39]
Moisture Stress Index	MSI	R_{1600}/R_{817}	[40]
Normalized Difference Water Index	NDWI	$(R_{860}-R_{1240})/(860+1240)$	[41]
Normalized Difference Infrared Index	NDII	$(R_{819}-R_{1649})/(R_{819}+1649)$	[42]

Similar changes in reflectance of isolated Sphagnum mosses under controlled conditions have been reported from other habitats including north temperate and boreal forests [15]. Van Gaalen (2005) found that reflectance spectra and photosynthetic yield of

Sphagnum changed in response to desiccation and that the Water Band Index (WBI) was significantly correlated with moisture content, but did not explore other moisture indices beyond 1000 nm. Vogelmann and Moss (1993) found that Sphagnum mosses exhibited, very pronounced water-related absorption features between 1000 and 1200 nm, that were not found in vascular plant reflectance, though the atmospheric window is partially closed in that region. The atmospheric window is a portion of the spectrum which does not get absorbed by atmospheric gasses/particles in the atmosphere allowing light to be reflected back to the sensor [37]. They also reported that the moss was generally less reflective than their reference vascular plant (white pine), however, on the basis of figures in the paper, once the moss was dried, it was more reflective than the reference vascular plant. This finding implies that in a spectrally mixed pixel, the intensity of mosses reflectance is contingent on their moisture content which influences the overall mixed pixel.

I.6 –Tissue Effects on Spectral Reflectance

Because of the unique morphology of mosses, the ability to differentiate them in high resolution spectra will likely be a result of differences between vascular and nonvascular plant tissues and how moisture interacts with leaf components to affect absorption and reflection in the NIR/SWIR region. Sphagnum moss leaves lack other vascular plant components such as xylem/phloem [43]. In addition, moss leaves are typically only one cell thick, and generally do not have stomata which facilitate gas exchange and function to control moisture loss [43]. Sphagnum mosses have specialized cells that transport water called hyaline cells, that function to retain water but are dead at

maturity, and chlorophyllose cells which contain chlorophyll for photosynthesis [44]. Water-saturated moss leaves strongly absorb radiation in the SWIR. In contrast, the large amount of cellulose/lignin in the intercellular mesophyll of vascular plant leaves influences how reflectance in the moisture bands differs from moss because of the structural obstacles in the light path that influence how light is reflected (returns to the sensor) [45-47].

I.7 – The Red Edge Region

A spectral region of particular interest in remote sensing of plants is known as the Red Edge (RE), the transition zone between red and NIR regions where rapid decline in absorption in the red progresses to reflectance in the NIR. The RE is useful for unique identifying characteristics of mosses compared to vascular plants. Bubier *et al* (1997) showed that several species of boreal wetland, temperate and forest mosses (Sphagnum, “brown”, and feather mosses) exhibited a different spectral shape and RE position (less abrupt red edge, more absorption in the green, less in the red, and pronounced water absorption features in the NIR) compared to vascular plants [45] (Figure 7). Various other studies of moss spectra produced similar results [8, 13-15, 45, 48]. Pigment absorption, leaf cell structure, and vitality all affect the RE region, and the RE parameters such as inflection point via first derivative are frequently used in the estimation of chlorophyll content [49-51]. The RE regions is thus a good potential region for classification purposes as they are distinct from vascular plants.

I.8 – Classification and Derivative Spectroscopy in Remote Sensing

Classification of mosses will be imperative to endmember unmixing. In my thesis research, analysis of endmember spectra is two-fold: mosses compared to vascular plants, and dry moss compared to saturated moss. Interpretation of imagery is contingent upon first determining the mixture of the signal (mosses, vascular plants, lichens, etc) and then the convolution of moisture content of mosses. Detection and identification of samples by investigating the collected spectra and comparing it to reference library spectra is a basic method of interpretation in spectroscopy. The principle of spectroscopy -a field originally developed in analytical and physical chemistry, but now applied to remote sensing of the environment- is founded on each type of material having a distinctive way of reflecting, absorbing, or emitting electromagnetic radiation [52]. Despite the differences in data acquisition between the controlled laboratory environment (homogenous samples, control of viewing angle, intensity and spectral distribution of light) and the challenges facing remote sensing (passive sensors using natural illumination, limited viewing angle, heterogenous mixtures of targets, spectral resolution, etc), derivative spectra can be used to reduce or eliminate background signals and resolve overlapping features [52-55]. Thus, matching between unidentified observed spectra and reference library spectra is possible since the spectral shape can be characterized by spectral derivatives (note that the derivative is only sensitive to shape, not magnitude), though controlled lab reference spectra are not always a great match to field collected spectra[52, 53, 56].

Nevertheless, derivative spectra has been used successfully for classification purposes as Bahrami and Mobasher (2020) demonstrated ~90% accuracy in

identification of unknown spectra using a Coding Based on Selected Threshold (CBSeT) method with Spectral Angle Mapper (SAM) and showed that the shape of spectra among species in the same family had the lowest spectral vector angles indicative of high similarity to within family species [57]. As the derivative spectra increases, spectral vector angles increase, implying an increase in capability for distinction among species [57]. In addition to classification techniques, spectral derivative approaches have also been employed in biophysical estimation methods, such as pigment analysis to determine chemical composition of leaves to track physiological changes in plant canopies, showing that indices using derivative spectra were more robust than broadband spectral indices (even in aquatic systems, where chlorophyll content is harder to estimate) [51, 53, 58]. Further, derivative spectra have been used to reduce atmospheric effects and spectral distortions due to variable sunlight which demonstrates the broad utility of derivative spectra [56, 59]. To better understand how moss influences arctic vegetation spectral signals, it is important to first establish endmember spectra and explore differences that can be extrapolated.

I.9 – Summary of Background Information and Significance

Understanding how mosses influence satellite derived indices in the Arctic will be a major advance to projecting and interpreting change in the future arctic. We know that moss reflectance changes depending on moisture content, but the question is how it is changing and to what extent it is driving spectral signatures in satellite imagery? More research is needed to elucidate how mosses influence satellite imagery and how that may impact NDVI (productivity) driven models. The results of this study will be particularly

timely as warming trends across the globe are exacerbated in arctic systems, because of their inherent geographical and surface properties [69]. The Arctic is currently warming at twice the rate of the global average, rapidly changing the tundra biome in diverse ways, where habitat shifts are complex and are heavily dependent on permafrost thaw and topography, among other physical and chemical characteristics [70-72].

As a result of widely varying environmental characteristics such as precipitation (rain and snow), vegetation community composition, permafrost, and warming trends across the tundra biome, understanding the ecological response to climate change projections is challenging [73-76]. Despite models that predict overall increasing precipitation in the Arctic, most of the increases are expected to fall as snow in winter and fall, as opposed to rain during the growing season, which can significantly hinder the available moisture to tundra plants and mosses [77]. Decreased growing season precipitation rates coupled with changes in precipitation patterns, increased evapotranspiration, thawing permafrost and subsequent lower water tables have the potential to seriously alter available moisture to mosses and tundra plants in the future Arctic [78-81]. Ecosystem models of how tundra will respond to these climate changes that use inputs from remote sensing will need accurate interpretation of those inputs for the best possible projections.

I.10 – Statement of Research Objectives and Hypotheses

The purpose of my thesis research is to evaluate the spectral changes that occur in mosses as a function of moisture content and find the best predictors for moisture content. For this research to be useful to real-world applications, classification of mosses

from mixed pixels will be crucial, thus (while beyond the scope of my thesis) regions for potential classification were also explored by comparing against vascular plant spectra. To build moss moisture-spectral index relationships, I conducted a lab-controlled drying experiment using field grown moss slabs during which spectral reflectance in the range from 350-2500 nm and moss moisture content were measured periodically as the moss dried down. Additionally, I examined vascular plant spectra *in situ* and compare them to moss spectra to search for unique spectral features for classification potential. Finally, I conducted a pilot study examining the effects of a short-term moisture fluctuation of *in situ* small-scale community-level vegetation on hyperspectral reflectance to test whether mosses can significantly drive community level spectra.

The following objectives were designed to explore the effects of moisture content on moss reflectance and to potentially classify mosses from vascular plants.

O1: Model the behavior of various spectral indices as a function of moisture content to find the best predictors.

O2: Explore moss and vascular plant spectra to find regions for potential distinguishing characteristics which can be used in classification analysis.

O3: Test whether mosses significantly drive community-level spectra in response to short-term moisture fluctuations.

II. Methods

II.1 - Site Description and Sample Collection

The study was conducted using samples collected at Imnaviat Creek (68°36'56.25" N, 149°18'21.17" W) near Toolik Arctic Field Station on the North Slope of Alaska. Tussock tundra, moist/wet acidic tundra, sedge tundra, and shrub tundra are just some of the communities present in this region and are representative of the vegetation communities across the Low Arctic (detailed vegetation community information can be found in Walker et al (2005) [60]). The low arctic has vegetation such as woody shrubs and willows that cannot grow in the high arctic where conditions are so harsh, that vegetation is typically limited to small flowering plants, grasses, mosses, and lichens. The dominant moist acidic tussock tundra community primarily consists of the graminoids *Eriophorum vaginatum* (tussocks) and *Carex bigelowii*, deciduous shrubs (*Betula nana* and *Salix pulchra*), evergreen shrubs (*Ledum palustre*, *Vaccinium vitis-idaea*, *Cassiope tetragona*), forbs (*Petasites frigidus*, *Rubus chamaemorus*) and bryophytes (mixed pleurocarpous moss spp. and *Sphagnum* spp.) and lichens (*Cladonia* spp. *Dactylina* spp.). The moss species found in mixed pleurocarpous communities (primarily *Hylocomium splendens* and various *Aulacomnium* spp. and *Dicranum* spp.) have either a cosmopolitan or circumpolar distribution and as a mixed community range in color from dull brownish green with hints of red to bright green depending on species present. The sphagnum species *Sphagnum capillifolium* [61] while *S. lenense* is limited primarily to North America/Greenland. Their color can range from green to orange and red depending photoprotective pigments present in the leaf tissue [43]. Despite their size,

these different moss species can form prominent homogenous patches in the inter-tussock spaces and at the tops of hummocks in addition to widespread heterogenous communities in the fine matrix of the understory[62].

Slabs of 12 orange colored sphagnum moss (OS) (n=12) (*Sphagnum fuscus* or *lenense*), 12 mixed pleurocarpous communities (MP, mostly *Hylocomium splendens*, with various *Aulacomnium* spp. and *Dicranum* spp. mixed in), and 14 red-colored sphagnum (RS, *Sphagnum capillifolium*) were harvested from the north side of Imnaviat Creek on a moderate slope ~ 920 m.a.s.l in July 2020 near peak season. The different moss samples were selected to be representative of moss communities found in these habitats (Toolik.alaska.edu). Reflectance scans (350-1,050nm) of the subset of each moss type (n = 5-8) were taken with internal halogen light source at 100% as baseline spectra with a UniSpec-SC spectroradiometer (PP Systems, Amesbury Massachusetts, USA) shortly after collection. Moss samples were moistened, wrapped up in cellophane to retain moisture, and shipped back to the laboratory at Florida International University (FIU).

II.2 - Sample Handling and Maintenance

Upon arrival, samples were placed in environmental growth chambers at ~15°C under fluorescent cool white light with 18-hour photoperiod and kept well hydrated using deionized (DI) water for several days prior to shipment to the University of El Paso Texas (UTEP) where a full solar range spectroradiometer (350-2,500nm) was available for our use. Slabs were prepared for shipment to UTEP by first carefully removing vascular plants from the moss and then cutting them to 10 x 10 x 8 cm squares and snugly

placing them into plastic food containers of the same dimensions. Once samples arrived at UTEP (overnight shipping), they were given a 14-day acclimation period prior to the start of the experiment and vascular plants that may have re-sprouted were removed. During this period, a 1,000 W LED full spectrum grow lamp (Parafacts Works, Shenzhen, China) was placed ~1 m above the samples to provide sufficient light to maintain moss photosynthesis without damaging the samples. Samples were watered daily with DI water.

II.3 - Instrumentation and Measurements

II.3a Moss Drying Experiment

To start the experiment, moss slabs were allowed to saturate with DI water for 2 hours, then excess moisture was drained off. At each measurement interval taken approximately every ~5%-10% of mass loss, mass, high resolution digital photographs, reflectance using the full range spectroradiometer, and moisture content were collected. Mass was measured using an AccuWeight Digital Scale and a VWR® P-Series Portable Balance and averaged. Moisture content was measured using an EC-5 soil moisture probe connected to a Decagon ECHO Check EC3528 (Decagon Devices, Pullman WA) and was collected in Analog to Digital RAW format to build my own calibration curves. Full range spectral reflectance was taken using a HR-1024i VIS-SWIR spectroradiometer from Spectra Vista Corporation (Spectra Vista Corporation, New York, USA) with the light source on high (spectral resolution: 3.3 nm, 700 nm; ≤ 9.5 nm, 1500 nm; ≤ 6.5 nm, 2100 nm; noise equivalence radiance: $\leq 0.8 \times 10^{-9}$ W/cm²/nm/sr @ 700 nm, $\leq 1.2 \times 10^{-9}$ W/cm²/nm/sr @ 2100 nm).

⁹ W/cm²/nm/sr @ 1500 nm, $\leq 1.2 \times 10^{-9}$ W/cm²/nm/sr @ 2100 nm). For each sample, four measurements (footprint ~ 4.6 cm²) per slab were taken and averaged to reduce variability across each specimen. Once the samples stopped losing any measurable weight, they were re-saturated (excess rinsed off) and two more days of the full suite of measurements were collected. Finally, samples were oven dried at 55 °C, and final dry weight and moisture content (for calibration) was recorded.

II.3b *Vascular Plant Spectra*

Vascular plant spectra were collected in the field at the Imnaviat creek site during the summers of 2020 and 2021 using the same HR-1024i VIS-SWIR spectroradiometer with the light source on high (for less noisy scans) and the leaf clip attachment engaged. Seven common arctic vascular plant species were measured; *Betula nana* (n=14), *Salix pulchra* (n=15), *Petasites frigidus* (n=5), *Vaccinium vitis-idea* (n=10), *Arctous alpina* (n=10), *Empetrum nigrum* (n=9), *Eriophorum vaginatum* (n=5) leaves were each measured haphazardly during peak season under ambient moisture conditions. The resultant data were compiled into a spectral library in the R statistical environment (R Core Team, 2017, Vienna, Austria) using the ‘hsdar’ package for comparison with the moss sample spectra [63].

II.3c *Community-level Rehydration Experiment*

In this *in situ* study conducted at Imnaviat Creek in July 2021, three 25 cm diameter plots at the tops of hummocks where sphagnum mosses (*Sphagnum capillifolium*, *Sphagnum lenense*, and *Sphagnum angustifolium*) had naturally dried out were selected. Using the HR-1024i VIS-SWIR spectroradiometer, plot-level, moss-level, and leaf-level reflectance measurements were taken before and after the addition of ~ 150 ml of water per plot to rehydrate the moss. After ~ 30-60 minutes (to allow the water to permeate the moss layer), plot-level, moss-level, and leaf-level measurements were repeated. Moss-level and leaf-level measurements were collected with light source on high and white reference.

II.4 - Analysis Approach

II.4a *Moss Drying Experiment*

Analyses were performed in the R statistical environment (R Core Team, 2017, Vienna, Austria) using the ‘hsdar’ package to analyze the high-resolution spectral data [63]. The spectra collected at each drying interval were divided into 10% moisture brackets. The four spectral scans for each replicate for each species were averaged before creating a spectral library (originally 2,888 scans were averaged to 722 spectral scans, ~ 240 per species during the drying experiment). The ‘vegindex’ function was used on the spectral library to extract an array of spectral indices. These indices were then tied to the experimentally collected supplementary data to manipulate the data frame to explore moisture-spectral index correlations and relationships. The indices which were

investigated here were: NDVI, WBI, NDWI, NDII, and MSI as described in table 1. It is important to note that NDWI refers to one of a minimum of two spectral indices concerned with water. One is $(\text{Green} - \text{NIR})/(\text{Green} + \text{NIR})$ which is useful for indicating the amount of water in a water body, and the one used here which is $(\text{NIR} - \text{SWIR})/(\text{NIR} + \text{SWIR})$ which provides information of moisture in the leaves of vegetation. The objective was to first determine that a correlation between moisture content and indices existed before determining the shape of the relationship. After determining that the relationship between various indices of interest and the moisture content were mostly non-linear, a mixed model repeated measures analysis was performed (with random effects on the replicates), both for individual moss types separately and all types grouped to determine which index performed best using the moisture content by percentage as the predictor or explanatory variable and the index as the response variable. Various models were tested, such as linear, decay, and sigmoidal functions such as the logistic and Gompertz functions. The shape of the relationship between the spectral indices and moisture content was generally sigmoidal in nature with some exceptions and the Gompertz function best fits the theoretical data distribution of the limits of these bounded indices which we expect to be sigmoidal in nature (either symmetric or asymmetric of the inflection point, logistic and Gompertz respectively).

First, the indices data frame was randomly split into training and testing datasets at 70% and 30% respectively. The ‘drc’ package in R, coupled with the ‘aomisc’ package (self-starters for nonlinear analysis) were primarily utilized. Models were generated using the training data and then validated using the testing data. Plots were created with the predicted values and the 95% confidence interval for visual interpretation. A linear

regression was performed between the observed and predicted spectral index values, and the R^2 was recorded. Akaike Information Criterion (AIC) was used to determine which model performed best for each species and index.

II.4b Moss and Vascular Plant Spectral Comparisons

Analyses were performed in R statistical environment (R Core Team, 2017, Vienna, Austria) using the ‘hsdar’ package with the high-resolution spectral data. Moss and vascular plant spectral scans were averaged by species and plant type and the resulting data frame was used to create a combined spectral library. To calculate the first and second derivative spectra, the ‘derivative.speclib’ function in the ‘hsdar’ package was used, and to produce less noisy derivatives, spectra were smoothed with the ‘Savitzky-Golay-Filter’ first [63]. Visual interpretation was used to identify the positions of the derivatives of interest based on the graphical illustration. Red edge parameters were also calculated using the ‘rededge()’ function in the ‘hsdar’ package to compare with the derivative spectra [63].

II.4c Community-level Rehydration Experiment

Hypothesis for Objective 3: Moisture content of the moss layer in a community-level plot (vascular and non-vascular plants intermixed) significantly drives spectral reflectance and influences key metrics such as NDVI, NDWI, and MSI. Vascular plants will not change in the short-term, but the community-level reflectance will change significantly in response to short-term rehydration, driven by the mosses.

The resultant data from the field study were compiled into a spectral library in the R statistical environment (R Core Team, 2017, Vienna, Austria) using the ‘hsdar’ package to extract indices and for graphical representation [63]. Boxplots were made comparing the two different moisture levels (wet and dry) of the three different plant groups (moss, vascular, and community-level). To determine whether significant difference in spectral indices (NDVI, NDWI, and MSI) between a dry and wet group existed, a paired student t-test (after normality was tested) was used between each moisture level for each plant group and then repeated for each index.

III. Results

III.1 - Spectral Profile at Varying Moisture Contents

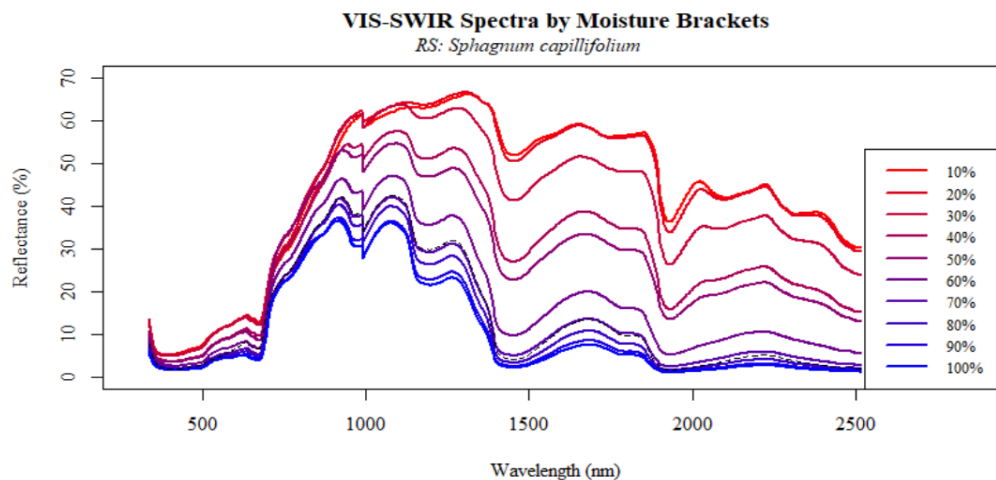


Figure 1: *S. capillifolium* (RS) spectra divided into moisture brackets. Note the small, but noticeable, differences in the green and red and large differences across the NIR and SWIR.

Both red *S. capillifolium* (RS) and orange *S. lenense* (OS) reflectance in the visible range, particularly in the red and orange (597nm-740nm), increased from ~4% to ~15% for RS and ~5% to 18% for OS as the moss dried (Figures 1, 2). Large difference

in the NIR/SWIR were observed as all three moss types dried (Figures 1, 2, 3). For both *S. capillifolium* and *S. lenense*, reflectance level from ~1,400nm to 2,500nm increases from ~ 5% when saturated to between 40%-60% as the moss samples lost moisture. Between ~1900nm-2500nm, large changes were observed when percent water is 60% and below, and three peaks in the region appear, becoming more pronounced when ~40% and below. Very similar prominent absorption peaks are present in the NIR for both sphagnum species. These peaks dissipate as the sample approaches complete desiccation.

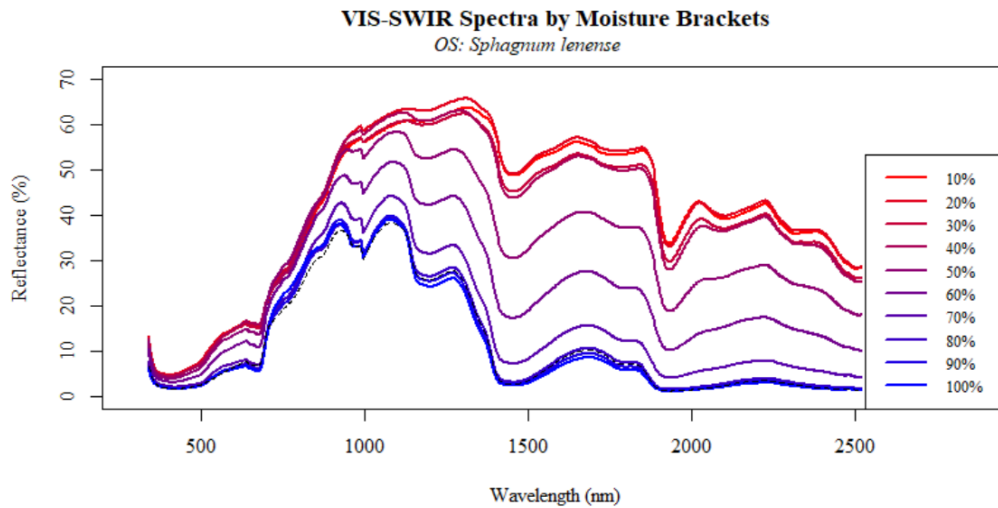


Figure 2: *S. lenense* (OS) spectra divided into moisture brackets. Note the small, but noticeable, differences in the green and red and large differences across the NIR and SWIR.

The spectra of the mixed pleurocarpous (MP) community did not exhibit as extreme changes in the visible or red edge region of the spectra as were noted in *S. capillifolium* and *S. lenense*. However, absorption in the green and red did slightly decrease with continued

drying.

Following the red edge transition zone

into the near

infrared,

separation of

moisture brackets

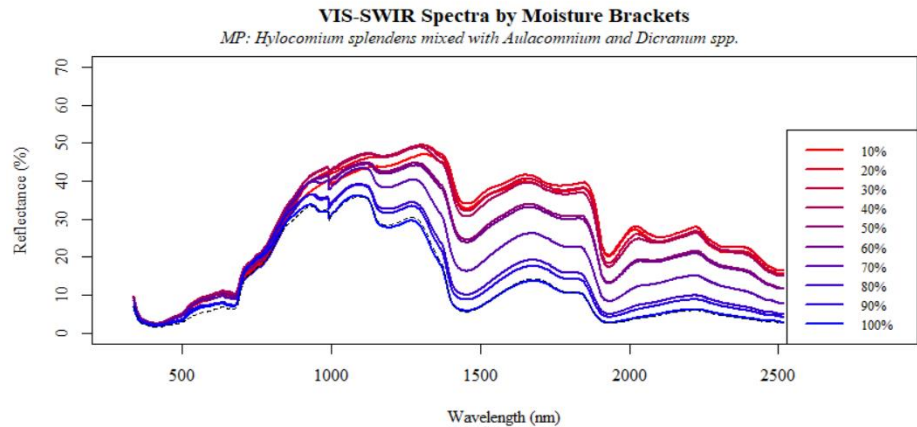


Figure 3: Mixed pleurocarpous community (MP) spectra divided into moisture brackets. Note the much smaller, but noticeable differences in the green and red and still large differences across the NIR and SWIR (not as large as sphagnum spp.)

was noted from approximately 900nm to 2500nm. The absorption peaks in the NIR and SWIR region were similar to those of *S. capillifolium* and *S. lenense*, though the magnitude of reflectance was not as high (~20% lower reflectance from the NIR to SWIR).

III.2 - Correlation of Moisture Content to Spectral Reflectance Indices

All four moisture indices were strongly correlated with moisture content (Table 2). *Sphagnum capillifolium* had the best correlations across all indices. For NDVI, *S. capillifolium* had the strongest correlation with *S. lenense* not far behind, and the mixed pleurocarpous moss had moderate correlations (Table 2). As moisture increased, NDVI increased most with *S. capillifolium* and *S. lenense* and only moderately with the mixed

pleurocarpous community. While the two NIR indices, WBI and NDWI, were strongly correlated with moisture for individual species and the combined mosses, the SWIR indices, MSI and NDII, were more strongly correlated.

Table 2: Summary of Spearman Rank Correlations of Spectral Indices. Results for each moss type (red sphagnum RS, orange sphagnum (OS), mixed pleurocarpous (MP), as well as all types grouped (Combined), for each spectral index, along with p-value of the Spearman correlation test.

Spectral Index	Property Sensed	RS	OS	MP	Combined	Normality By Group	p-value
NDVI	Greenness	0.83	0.73	0.57	0.65	N,N,Y, N	2.2E-16
WBI	Moisture	-0.91	-0.77	-0.80	-0.80	N,N,N,N	2.2E-16
NDWI	Moisture	0.91	0.80	0.85	0.81	N,N,N,N	2.2E-16
NDII	Moisture	0.91	0.83	0.87	0.84	N,N,N,N	2.2E-16
MSI	Moisture	-0.91	-0.84	-0.87	-0.85	N,N,N,N	2.2E-16

III.3 – Nonlinear Modeling of Indices as a Function of Moisture Content

The parameters listed in Table 3 correspond to the logistic four parameter equation, $Y=c + ((d-c)/(1+\exp(-b(X-e))))$ and the Gompertz four parameter equation is $Y=c+(d-c)\exp\{-\exp[-b(X-e)]\}$ where coefficient 1, 2, 3, and 4 corresponding to b, c, d, and e respectively (see table 3 for description of each coefficient, logistic model shown). AIC values were compared across the row for each index to determine which function best modeled the index behavior (the lower the AIC, the better the model). Given the theoretical distribution of the bounded indices being sigmoidal in nature, the logistic and

Gompertz models performed best for each index, with the Gompertz model generally providing the better model (Table 4). The AIC scores cannot be compared across species or spectral indices, only across the same species and index. Based on the regressions shown in Figure 4 and 5 using the test data however, it appears that NDWI and NDII performed best among indices when predicting the spectral index given the moisture content for all individual species as well as for all the mosses combined.

NDWI has the added benefit of having positive and negative values at the extreme ends of moisture content. For example, to generalize for both *S. capillifolium* and *S. lenense*, NDWI values that are negative correspond with dry moss (<50% moisture content) and values which are positive corresponded with wet moss (>50% moisture) (Figure 4). This rule can be useful for remote sensing because it can indicate whether moss are wet or dry at their surface, and sphagnum species in particular strongly shift spectral characteristics once they reach ~50- 60% moisture content, as in III.1 and observed by May et al (2018) [16]. All moisture indices were significant in predicting moisture content of the mixed pleurocarpous moss, but NDWI again appeared to performed best (Figure 5).

The logistic model for mixed pleurocarpous NDVI did not perform well because there was large variation and small changes relative to moisture content, but modeling it with a linear model did produce significant results which is in agreement based on previous studies [16] (results not shown). However, for *S. capillifolium* and to a lesser extent *S. lenense*, NDVI did have a significant relationship with moisture content and the Gompertz model did best. WBI and MSI performed well at very high moisture contents

but had heteroskedastic behavior at low moistures for all moss communities (Figure 4 & 5) whereas NDWI and NDII performed reasonably well across the whole curve.

Table 3: Summary of Nonlinear Logistic Models. Results for each moss type *S. capillifolium* - red sphagnum (RS), *S. lenense* - orange sphagnum (OS), mixed pleurocarpous (MP), as well as all types grouped (mixed moss = MM), for each spectral index. **** denotes all parameters were 0.0001 significant, ***(n) signifies that three parameters were *** significant, and one was a different level of significance. *** = 0.001, ** = 0.01, * = 0.05, '.' = 0.1. Coefficients for the logistic formula are listed and their corresponding species are to the right. Residual Square Error = RSE, Lack-of-Fit = LoF, Observed vs Predicted = O vs P

Spectral Index	Logistic 4 par equation	RS	OS	MP	MM	Coefficient 1 Slope of inflection pt	Coefficient 2 Lower asymptote	Coefficient 3 Higher asymptote	Coefficient 4 ED50	
NDVI	Parameter p-value	****	***(**)	***(0)	***(**)	-10.7637164	0.472049	0.7432493	0.4244433	RS
	RSE	0.058	0.097	0.8	0.11	-14.82607	0.333415	0.628463	0.52022	OS
	LoF p-value	0.19	0.62	0.97	0.55	-21.4231247	0.4048372	0.5335237	0.599486	MP
	AIC	-400	-230	-311	-636.3	-10.346728	0.401152	0.652931	0.521862	MM
	O vs P adj R ²	0.72	0.52	0.25	0.38					
	O vs P param p-value	****	****	****	****					
	O vs P p-value	0	0	0.0001	0					
WBI	Parameter p-value	****	****	***(*)	****	5.483199	0.829819	1.236585	0.415002	RS
	RSE	0.058	0.033	0.039	0.0717	14.241342	0.907855	1.176796	0.537161	OS
	LoF p-value	0.81	0.04	0.55	0.5	4.724458	0.910096	1.137342	0.774766	MP
	AIC	-401	-306	-518.9	-1001.7	8.2788696	0.8976756	1.1634439	0.5423116	MM
	O vs P adj R ²	0.76	0.83	0.84	0.73					
	O vs P param p-value	***(**)	***(**)	****	***(0)					
	O vs P p-value	0	0	0	0					
NDWI	Parameter p-value	****	****	***(*)	****	-6.829037	-0.200366	0.199978	0.47759	RS
	RSE	0.0436	0.0558	0.0294	0.07	-12.385312	-0.200462	0.111059	0.536963	OS
	LoF p-value	0.6	0.36	0.25	0.48	-5.4977767	-0.2002599	0.0741198	0.7124077	MP
	AIC	-481	-372.4	-597.3	-1024	-7.66242	-0.197433	0.129228	0.558243	MM
	O vs P adj R ²	0.9	0.86	0.88	0.76					
	O vs P param p-value	***(0)	***(*)	****	****					
	O vs P p-value	0	0	0	0					

Table 3 continued: Summary of Nonlinear Logistic Models. Results for each moss type *S. capillifolium* - red sphagnum RS, *S. lenense* - orange sphagnum (OS), mixed pleurocarpous (MP), as well as all types grouped (mixed moss = MM), for each spectral index. **** denotes all parameters were 0.0001 significant, ***(n) signifies that three parameters were *** significant, and one was a different level of significance. *** = 0.001, ** = 0.01, * = 0.05, ‘.’ = 0.1. Coefficients for the logistic formula are listed and their corresponding species are to the right. Residual Square error = RSE, Lack-of-Fit = LoF, Observed vs Predicted = O vs P

Spectral Index	Logistic 4 par equation	RS	OS	MP	MM	Coefficient 1 Slope of inflection pt	Coefficient 2 Lower asymptote	Coefficient 3 Higher asymptote	Coefficient 4 ED50	
NDII	Parameter p-vau	****	****	****	****	-7.905406	-0.253042	0.620332	0.463232	RS
	RSE	0.0748	0.0848	0.0602	0.1319	-12.405603	-0.23061	0.55341	0.550445	OS
	LoF p-value	0.32	0.34	0.1	0.48	-6.235663	-0.245487	0.419113	0.695122	MP
	AIC	-327.7	-264.7	-392.2	-496.6	-8.190237	-0.240868	0.528313	0.553465	MM
	O vs P adj R^2	0.96	0.94	0.91	0.85					
	O vs P param p-value	***()	***()	***()	****					
	O vs P p-value	0	0	0	0					
MSI	Parameter p-vau	****	****	****	****	10.574008	0.219046	1.571886	0.386119	RS
	RSE	0.1663	0.2045	0.144	0.2258	13.283107	0.244714	1.585135	0.499531	OS
	LoF p-value	0.46	0.0345	0.08	0.053	6.916012	0.391178	1.609046	0.586677	MP
	AIC	-100.5	-37.4	-142.5	-52.2	9.375027	0.292081	1.586862	0.485024	MM
	O vs P adj R^2	0.92	0.88	0.9	0.84					
	O vs P param p-value	***(.)	***(*)	***(**)	****					
	O vs P p-value	0	0	0	0					

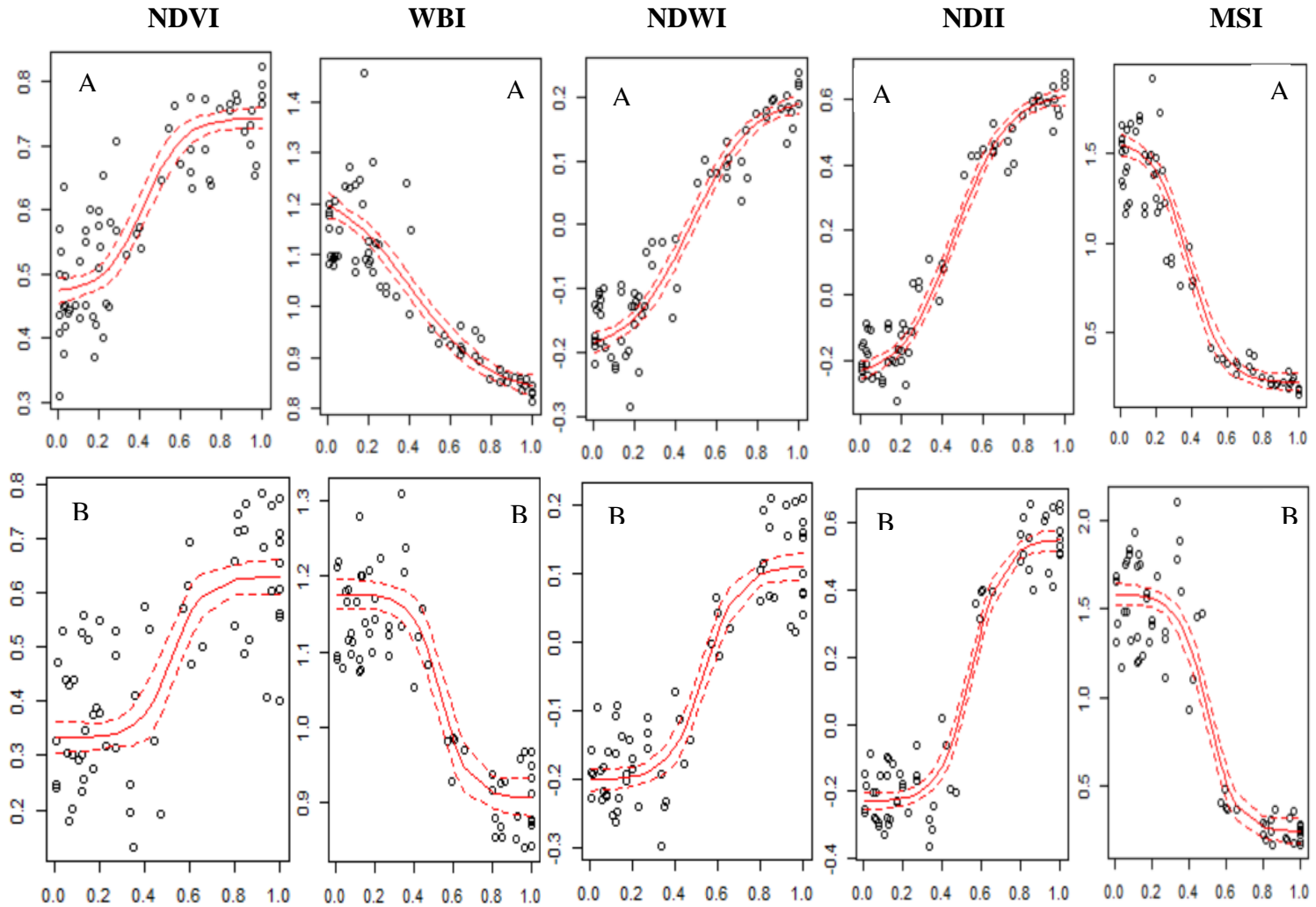


Figure 4: Gompertz model predictions on testing dataset for *S. capillifolium* (red sphagnum) (A) and *S. lenense* (orange sphagnum) (B). X axis is moisture content and Y axis corresponds to the values for each respective index. Predicted model and C.I 95% in red.

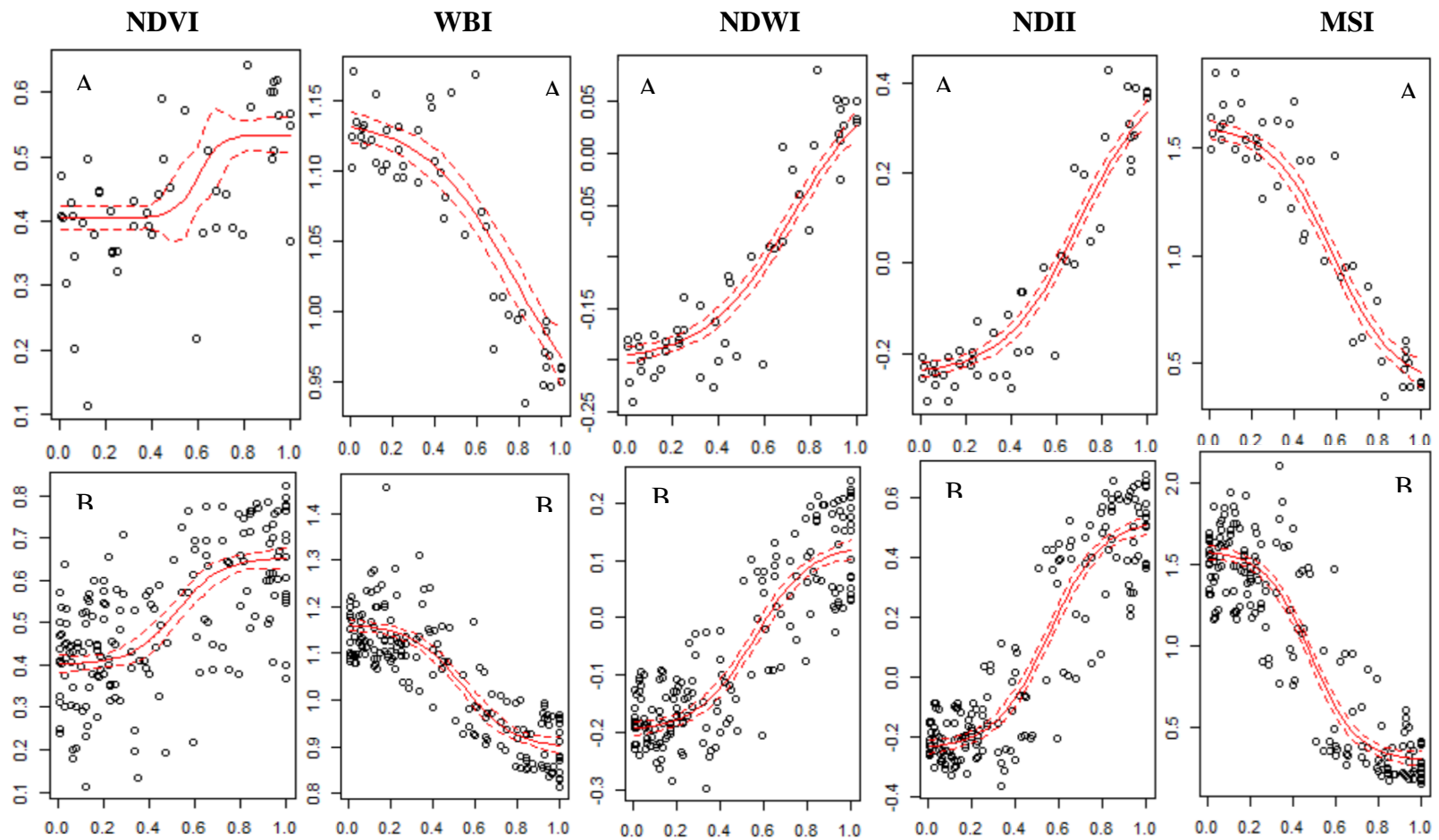


Figure 5: Gompertz model predictions on testing dataset for mixed pleurocarpous moss (MP) (A) and mixed moss (MM) (B). X axis is moisture content and Y axis corresponds to the values for each respective index. Predicted model and C.I 95% in red.

AIC Values

Indices/Models		Linear	Decay	Logistic	Gompertz
RS	NDVI	-375.6	-380.1	-400.2	-400.2
	WBI	-393.7	-396.8	-401.8	-400.4
	NDWI	-460.7	-459.6	-485	-487.2
	NDII	-267.2	-270	-329.5	-334.7
	MSI	-28.9	-54.2	-104.9	-98.4
OS	NDVI	-219.6	-216.2	-229.7	-229
	WBI	-275.6	-271.4	-306.5	-305.8
	NDWI	-328.6	-319.4	-372.8	-374.2
	NDII	-169.3	-161.6	-266.2	-264.9
	MSI	24	26.8	-37.4	-35.4
MP	NDVI	-317.3	-313.7	-315.6	-314.1
	WBI	-504.5	-500	-518.6	-500.5
	NDWI	-546.1	-535.4	-591.1	-592.5
	NDII	-311	-301.2	-382.7	-382.7
	MSI	-102.5	-98.8	-132.9	-131.4

Table 4: AIC summary chart for all three species and all five indices. RS = *S. capillifolium*, OS = *S. lenense*, MP = mixed pleurocarpous community.

III.4 - Moss and Vascular Plant Spectral Comparisons

III.4a – Investigating Derivative Spectra

Spectra for each species were averaged together (RS: n = 80, RS.D: n = 96, OS: n = 62, OS.D: 85, MP: n = 58, MP.D: 85, MM: n = 200, VP: n = 68) and were plotted to visualize moss under hydrated (>70%) and desiccated (<30%) conditions and vascular spectra under moist field conditions (Figure 6).

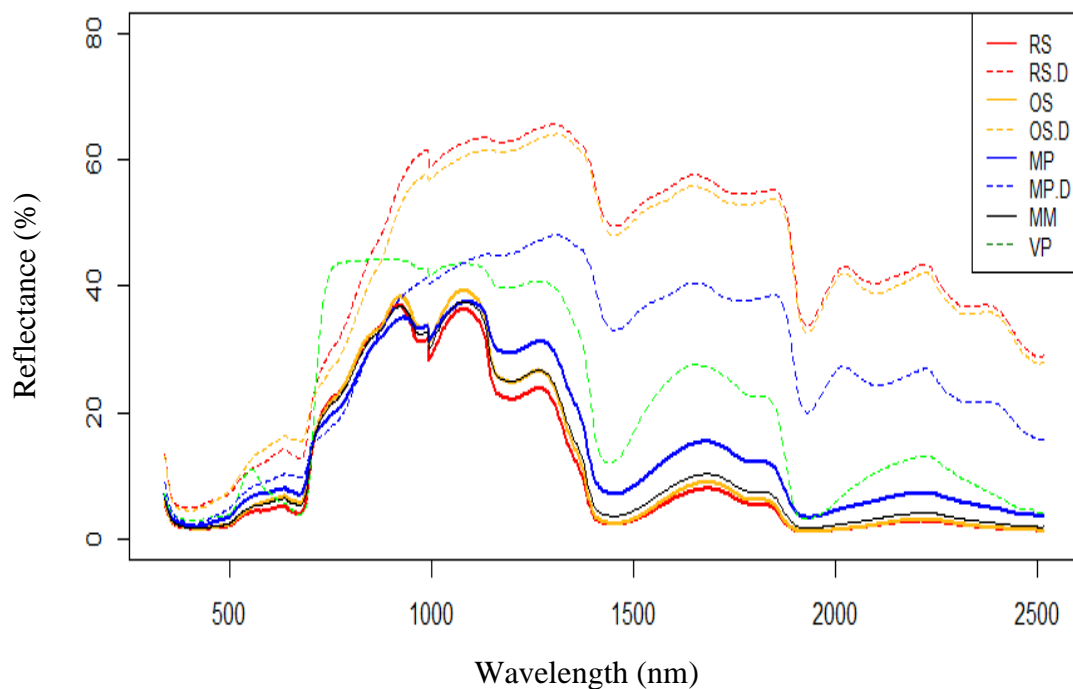


Figure 6: Average spectral signature by group. RS = red sphagnum, RS.D = red sphagnum dry, OS = orange sphagnum, OS.D = orange sphagnum dry, MP = mixed pleurocarpous, MP.D = mixed pleurocarpous dry, MM = all moss types combined, and VP = vascular plants.

Given the similarities in the three moss community spectra, spectral reflectance scans (n = 200 for wet mosses, n = 266 for dry mosses) of moss samples (all three communities combined and vascular samples (n = 68) (all 7 species combined) were averaged together, and 95% confidence intervals were calculated and plotted (Figure 7).

Upon visual inspection, the red edge leading into the NIR region was selected for further analysis because of the obvious difference in slope between the moss and vascular plants.

The raw, first and second derivative spectra were compiled, and the full range spectra were reduced to 600nm to 1000nm and plotted for better visualization (Figure 8).

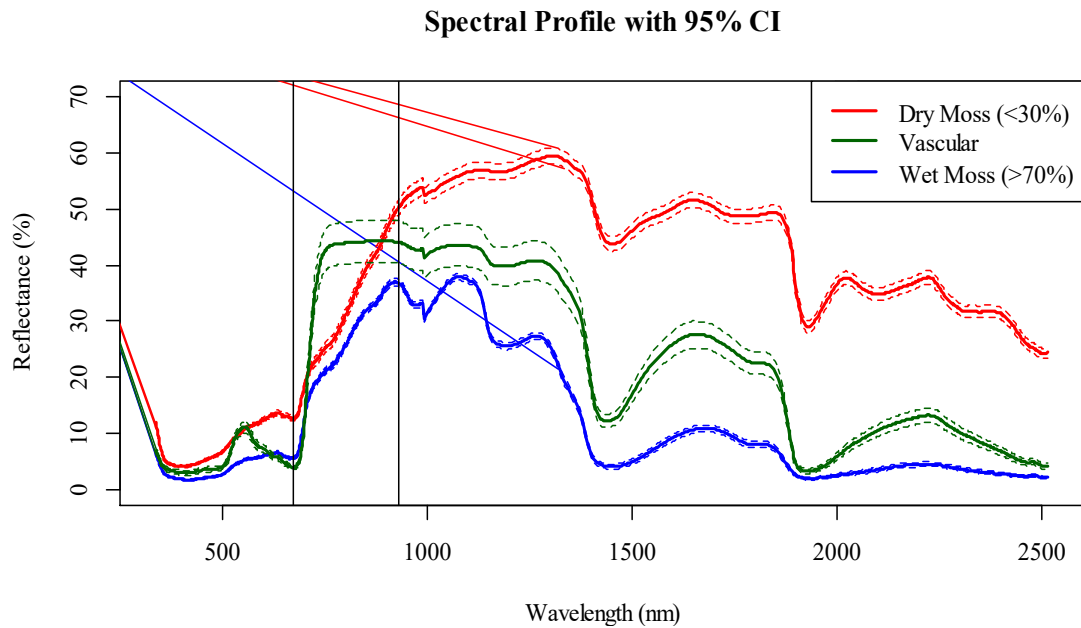


Figure 7: Average spectral profile of moss and vascular plants w/ 95% confidence intervals. Vertical black lines show the region of interest for further analysis.

The first derivative reaches its peak and the second derivative is equal to zero when the blue vertical line (moss) is centered at 697nm and the green vertical line (vascular) is centered at 709nm, demonstrating a significant shift in the location of the inflection point between the vascular plants and mosses.

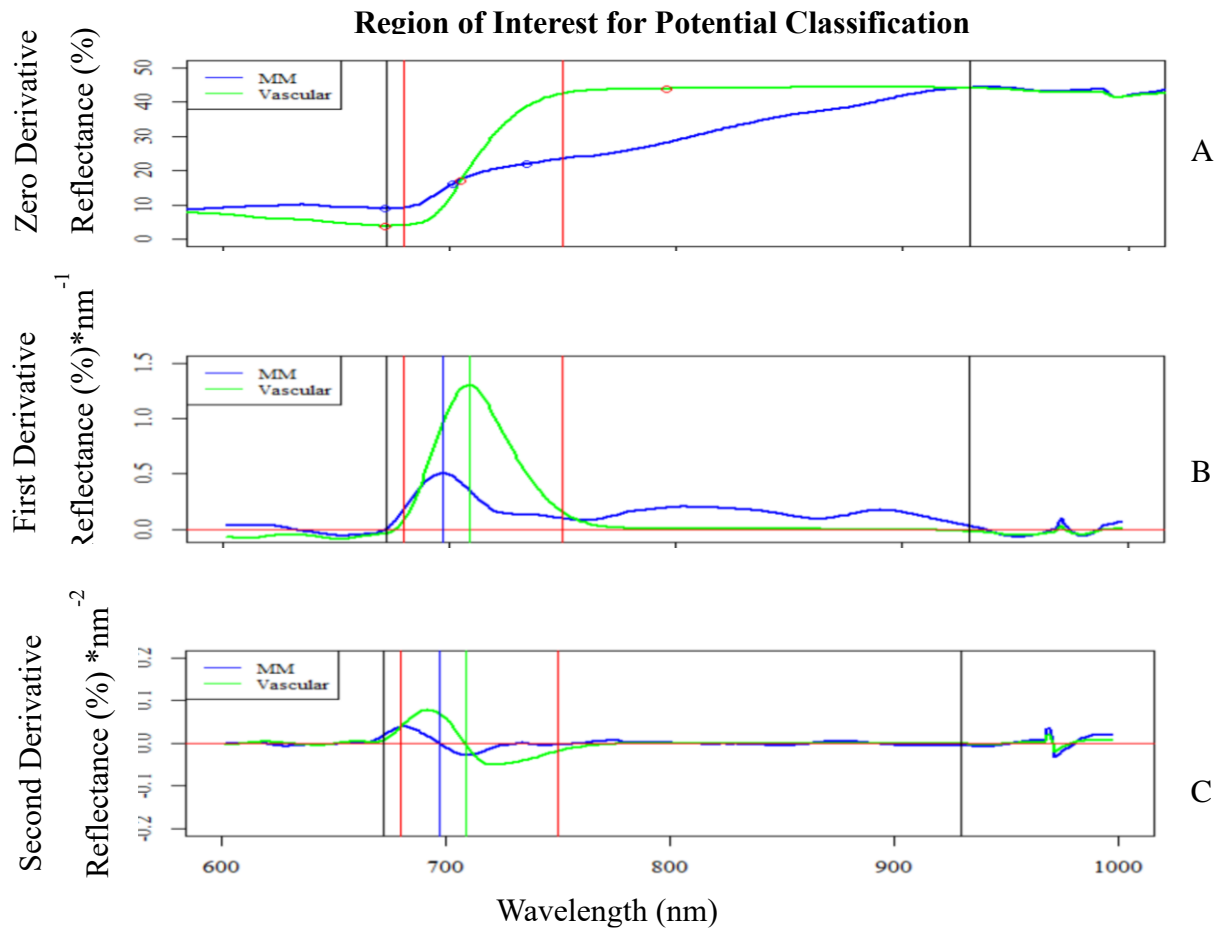


Figure 8: Zero derivative spectra (A) and first (B) and second derivative (C) spectra for mixed mosses (MM, blue) and Vascular Plants (Vascular, green). In A, the blue and red circles are the red edge minima, inflection, and shoulder (as calculated by 'hsdar::rededge()'). The red horizontal line is set to $y = 0$ to visualize where inflection point is found.

The difference in the shifted red edge inflection point (REIP) of moss and vascular plants in this experiment was 12nm. Furthermore, the first derivative of the vascular plants remaining at zero corresponds with the plateau in the raw vascular spectra after the red edge leading into the NIR. However, the first derivative of the moss remains positive from ~ 680nm all the way to ~930nm, corresponding with the increasing slope of the zero-derivative spectra of mosses from the red edge to the NIR. Given these two separating features to distinguish between endmember spectra of moss and vascular plants, differentiation between spectra and identification of unknown spectra is likely.

III.4b – Investigating Red Edge Parameters

I calculated the red edge parameters for all three moss types combined and for all vascular plant species combined using a different method (rededge function in hsdar) for comparison. The moss red edge shoulder position (RESP) occurred at a significantly lower wavelength with

average RESP ~ 723.5nm, whereas the average vascular plant red edge shoulder position was ~ 778.0nm (Figure 9). When the moss types were compared among each other, the

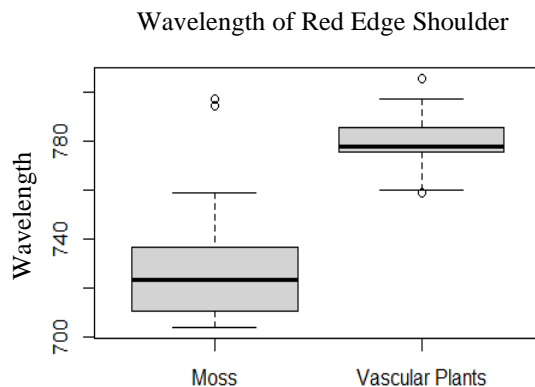


Figure 9: Boxplot comparing moss and vascular plant RESP.

RESP of the mixed pleurocarpous community mean was ~ 719.5nm, OS mean was ~729nm, and RS mean was ~ 727nm (Figure 10).

The RESP was chosen because the difference between vascular and moss samples was greatest compared to REIP and the red edge minima. Interestingly, the REIP which was determined via derivative spectra as previously discussed, and the REIP calculated

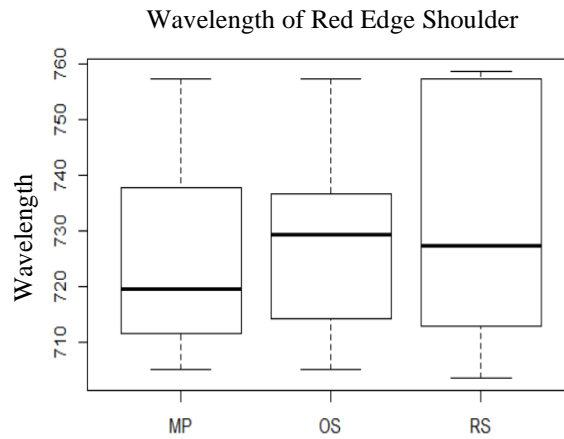


Figure 10: Boxplot comparing the red edge shoulder of MP (n=136), RS (n = 151), and OS (n = 141).

by the 'rededge()' function were slightly different, with the automated calculation for moss and vascular plants occurring at 701nm and 704 nm respectively, showing a much narrower range. This is likely the result of the 'rededge()' function being built under

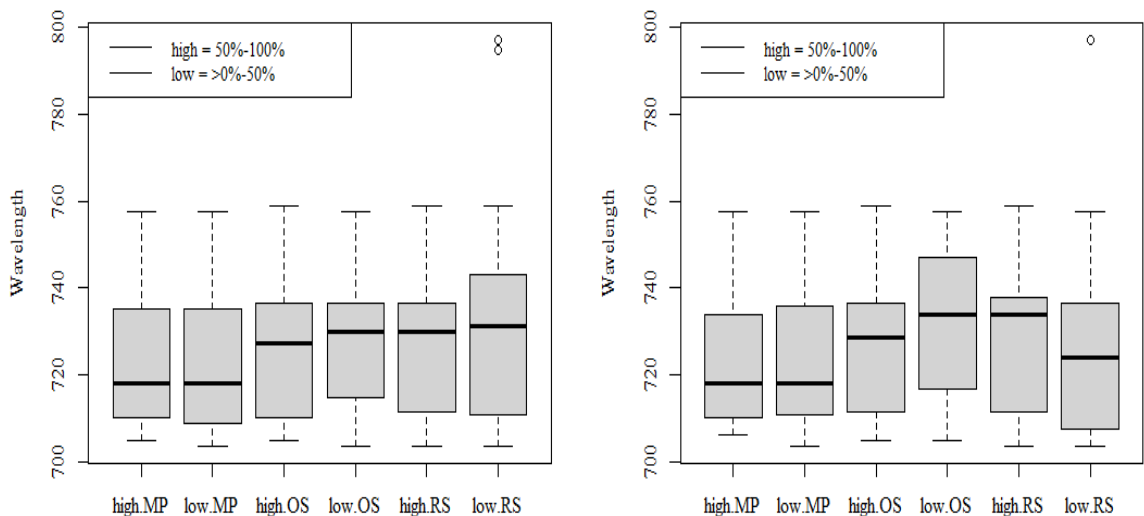


Figure 11: Boxplot comparing different amounts of high and low moisture content between the three different communities. High moisture >50%-100%, low moisture <0%-50% (left), High moisture >80%-100% low moisture <0%-20% (right).

spectral assumptions for vascular plants, whereas we can see that moss spectra in this range differs significantly (Figure 5). RESP was largely unaffected by moisture status (except at extreme differences), which is useful as an identifier of moss regardless of hydric status (Figure 11).

III. 5 – Evaluation of Potential Changes in Moss Spectra in Response to Shipping and Handling

Due to the life altering Covid-19 pandemic, the original planned experiment for my thesis was not able to be carried out in the field as intended. That experiment would have been comparable the pilot community rehydration study of 2021. As a result of mandatory quarantine procedures from the State of Alaska and Toolik Field Station, my 2020 field season was shortened to only 11 days instead of 90+ days. The constraints of time and unfortunate bad weather in the field during my stay necessitated that another experiment be devised that would use lab measurements of field collected samples. Those samples, replicate slabs of three moss communities were collected under field moisture conditions and scanned for VIS and NIR reflectance spectra prior to shipment to the lab at FIU. The samples received no light for several days during shipping while being exposed to an unknown range of temperatures. Samples were then placed in growth chambers for a few days under simulated field light and temperature conditions to recover from shipping. Samples were then exposed to one day of darkness during shipping to the UTEP followed by two weeks under grow light spectrum prior to the initiation of the drying experiment.

III.5a – Spectral Indices Evaluation

WBI was used to assess the moisture content of pre-shipment samples, collected, and scanned under field moisture conditions, and was found to have similar WBI when post-shipment mosses were ~ 65-80% saturated (Figure 12a), thus post-shipment samples were subset from 65-80% saturation. NDVI was used to assess if there were any spectral shifts in greenness associated with shipping and recovery. Comparing NDVI of both samples demonstrated that all three moss communities had significantly higher NDVI post-shipment (Figure 12b).

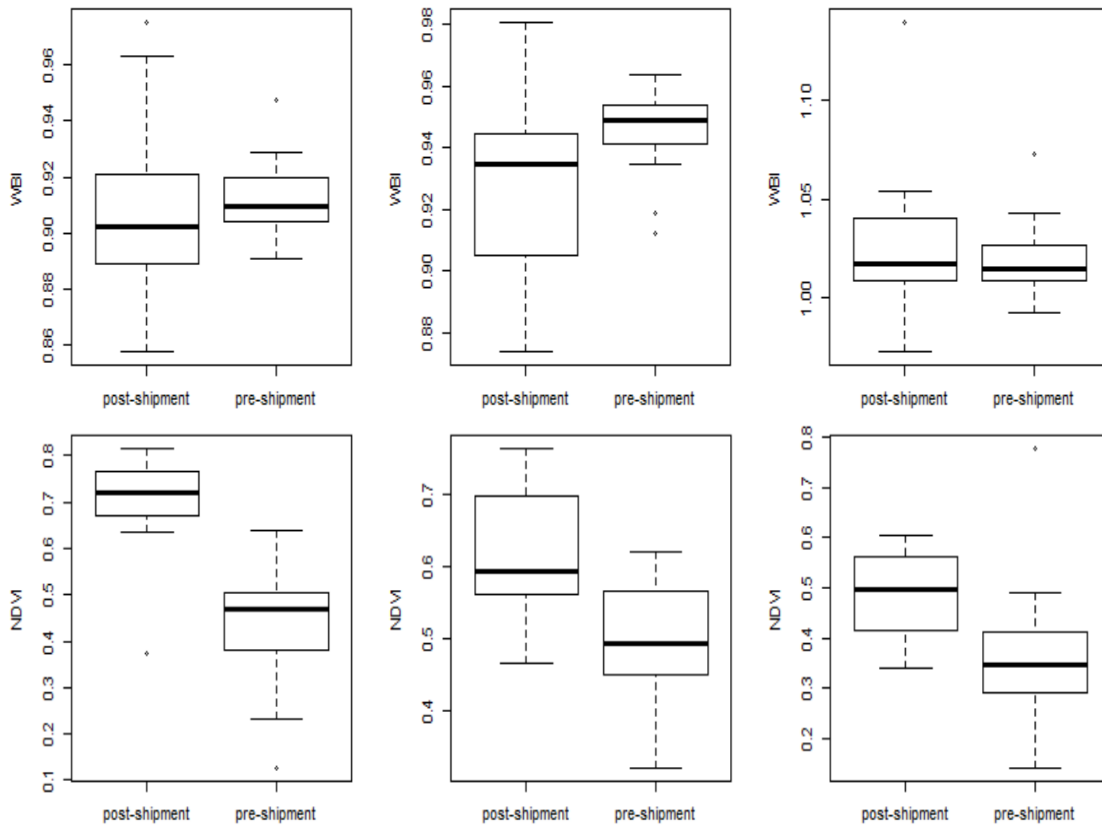


Figure 12: (12a- top row) WBI boxplot comparison of pre and post shipment. (12b- bottom row) NDVI boxplot comparison of pre and post shipment. For both top and bottom, from left to right is red sphagnum (RS), orange sphagnum (OS), and mixed pleurocarps (MP).

This was very likely because the samples were collected in the field at slightly above freezing temperatures towards the end of the growing season and placed into a warmer environment with subdued lighting and ample moisture thus encouraging growth. Previous studies have shown that *Sphagnum* species from the Toolik region are photoinhibited under open light conditions [65, 66]. The increased greenness of the samples post-shipment likely represents reduction and photoinhibition and loss of photoprotective pigments typically found in tundra grown *Sphagnum*. As a result, caution should be taken when considering the pigmented portion of the spectra (400nm-700nm), however, the NIR and SWIR portions of the spectra should theoretically not be negatively impacted because those portions of the spectra are much more sensitive to the attenuation of light of water molecules. Whether the NDVI differences observed are a result of sample size is unknown (pre-shipment: n =5-8 vs post-shipment: n = 12-14).

III.5b – Red edge parameters

There was a large difference in the RESP between post-shipment (mean ~ 725nm) and pre-shipment moss (mean ~ 760nm) (Figure 13). The difference in pre and post shipment moss may be the result of shipping/handling and growing conditions as

described
in III.5.

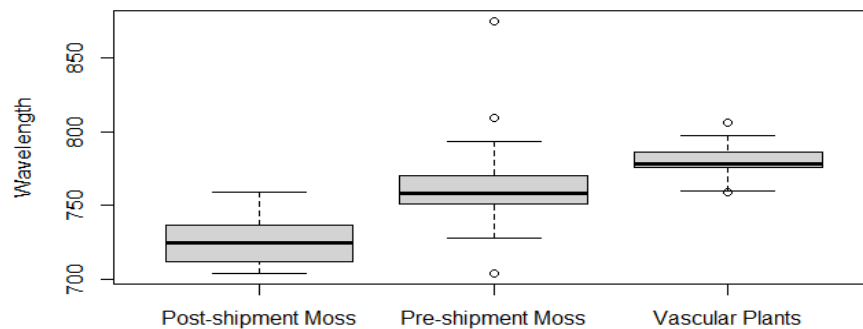
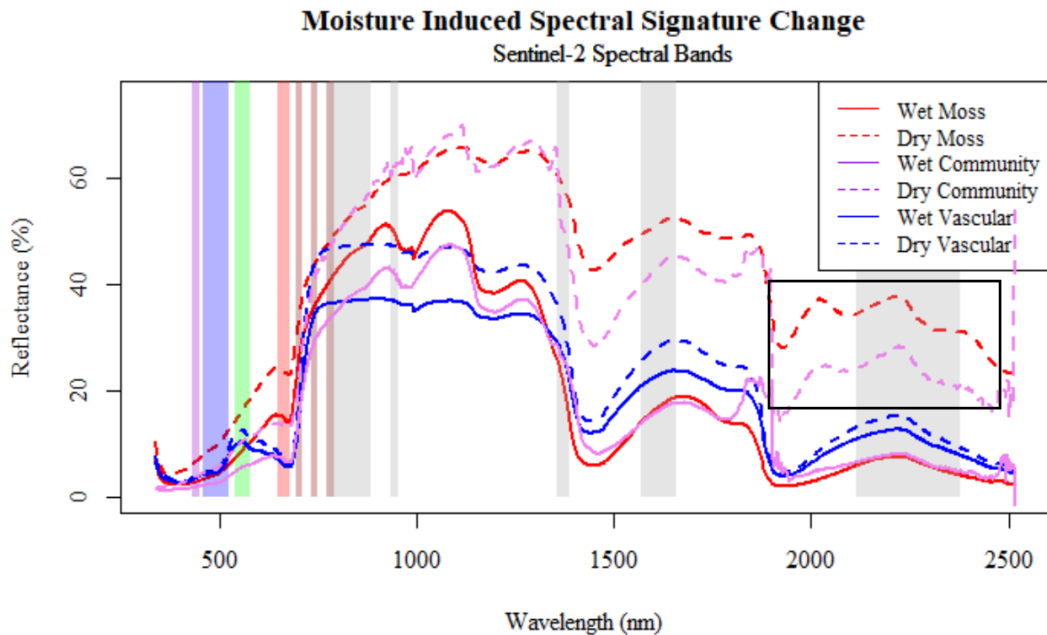


Figure 13: Boxplot comparing the pre-shipment moss (n = 50), post shipment moss and vascular plants (n=68).

III.6 – Community-level Rehydration Experiment

In situ Community-level, moss-level, and leaf-level spectral reflectance were collected for three different moss species (n=3) and each group of measurements were averaged together (moss, vascular, and mixed at both moisture levels) (Figure 14). Both moss and vascular spectra were similar to the lab collected spectra, although the mosses differed in the VIS more than in the *in-situ* samples with higher reflectance % at both wet and dry conditions. The *in situ* vascular spectra surprisingly did show that short-term moisture changes could be detected in the NIR, but the REIP appeared unchanged. The difference between dry and wet Community-level spectra, indicated that mosses were significantly driving the community-level spectral signature because the three peaks in



the SWIR (1,900nm-2,500nm) appear to large degree in the dry moss and to a lesser degree in the dry community-level spectra, while the vascular plants in that region do not change. However, when wet, both moss and community-level spectra decrease in intensity, and the three peaks present in the SWIR disappear. The community-level spectrum appears slightly jagged because it was collected under ambient sunlight conditions with troughs likely from atmospheric absorption, whereas the vascular and moss spectra were collected with a constant light source. The shape of the moss spectra, both wet and dry, may have differed slightly because of the time of year and growing conditions in which the spectra were collected *in situ* vs collected for the lab experiment.

Indices were derived from the spectra for further analysis. NDVI of the the moss samples changed significantly (p -value = 0.006469, $n = 3$, mean diff = 0.13) and community-level samples changed moderately (p -value = 0.08, mean diff = 0.11) in response to rehydration as determined by a paired Student t-test (Figure 15). Both the

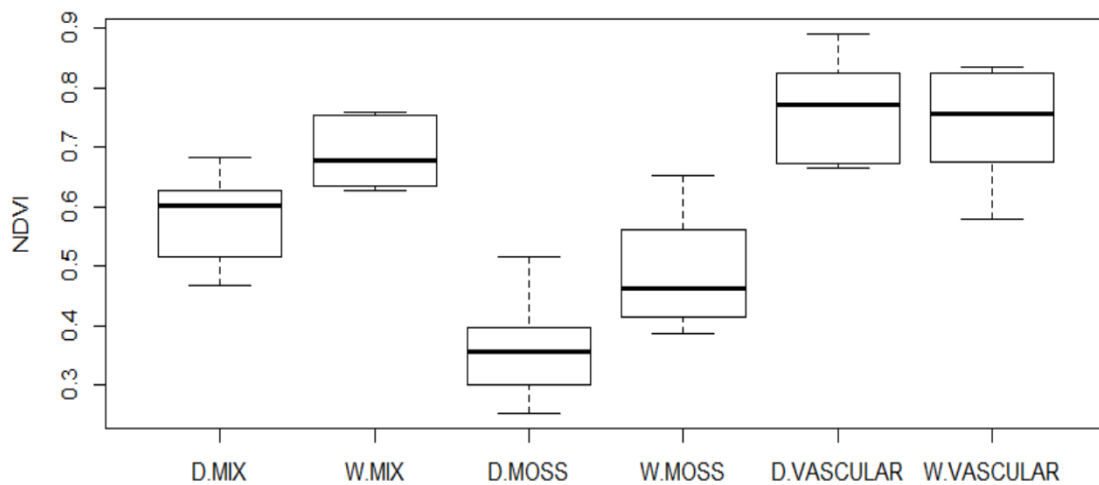


Figure 15: Boxplot showing NDVI differences between wet (W) and dry (D) conditions of the three groups (Mix or community, moss, and vascular plants). Vascular plants remain unchanged ($p > 0.05$), but the moss and community-level increase significantly ($p < 0.05$) with the addition of moisture.

community and the moss NDVI increased following the addition of water. However, NDVI of the vascular plant samples was unaffected by the short-term moisture change (p-value = 0.4138, n = 3, mean diff = 0.03). Given that NDVI values in tundra are already low, a change in 0.1 can be mistaken for increases in LAI and green biomass used for phenological studies when in fact, moisture content of mosses were likely driving the change. This result indicates that timing of remote sensing and investigating the moisture indices is crucial for accurate interpretation of spectra in arctic regions where mosses may drive the spectral signal.

Likewise, NDWI of the community and the moss samples also increased significantly (p-value = 0.03335 and 0.001145 respectively, n = 3, mean diff = 0.12 and 0.17 respectively) in response to the addition of water as determined by paired student t-test (Figure 16). However, NDWI of the vascular plants was again unaffected by the short-term moisture change (p-value = 0.554, n = 3, mean difference = 0.002).

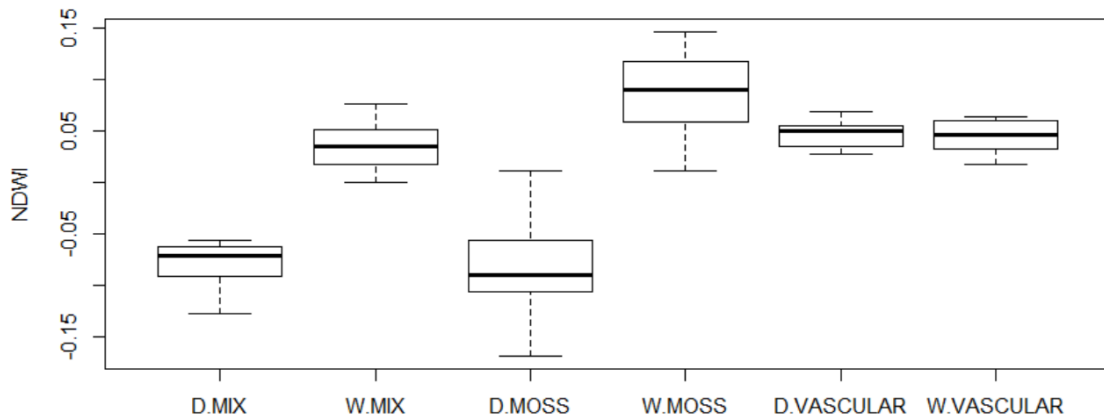


Figure 16: Boxplot showing NDWI differences between wet (W) and dry (D) conditions of the three groups (Mix or community, moss, and vascular plants). Vascular plants remain unchanged ($p > 0.05$), but the moss and community-level increase significantly ($p < 0.05$) with the addition of moisture.

MSI of the community and moss decreased significantly (p -value = 0.021 and p -value = 0.001 respectively, $n = 3$, mean diff = -0.41 and -0.64 respectively) in response to rehydration as determined by paired student t -test (Figure 17). However, MSI of the vascular plant samples was unaffected by the short-term moisture change (p -value = 0.5937, $n = 3$, mean diff = 0.01).

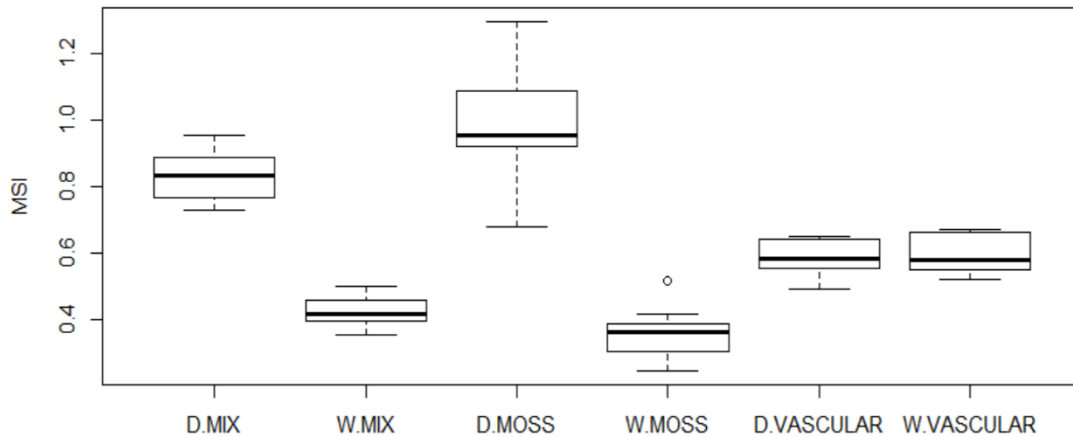


Figure 17: Boxplot showing MSI differences between wet (W) and dry (D) conditions of the three groups (Mix or community, moss, and vascular plants). Vascular plants remain unchanged ($p > 0.05$), but the moss and community-level decrease significantly ($p < 0.05$) with the addition of moisture.

III. Discussion

III.1 – Spectral Reflectance of Mosses During Drying

Overall, for the three moss communities, large increases in the NIR and SWIR were observed as the mosses dried. Changes in the NIR and SWIR region of moss spectra have mainly been attributed to physical changes in the plant canopy and are the result of moss hyaline cells releasing large amounts of water [11]. The spectral changes observed across the entire spectra compare very well with the work of Harris et al. (2005) [48]. These results corroborate results from experiments using different species of sphagnum

from different habitats, demonstrating that despite small differences in overall spectra, *Sphagnum* spp. as a group show similar spectral changes when drying and are distinct from that of vascular plants [8, 13-15, 45, 48]. In comparison, the red edge slope of the mixed pleurocarpous community appear to have a change in concavity not seen in Bubier et al (1997), though other experiments used homogenous *H. splendens* whereas mine was predominantly *H. splendens* and a mixture of different species [45, 82]. However, overall, the shape of the red edge did not change (the amount of reflectance % did) in response to moisture fluctuations which enabled identification of a potential classification region.

III.2 – Modeling behavior of spectral indices and moisture content of mosses

For the Spearman rank correlation, Water Band Index (WBI) and Moisture Stress Index (MSI) values were very similar to those in Harris et al (2005), although in Harris et. al. (2005) WBI was more strongly correlated and here MSI was more strongly correlated, but the sphagnum species in each study differed [48]. This result is in agreement with May et al. (2018) who found that NDVI of two *Sphagnum* species significantly decreased in response to moisture loss, while the mixed pleurocarpous community decreased, but to a far lesser extent [16]. While the two NIR indices, WBI and NDWI, were strongly correlated with moisture for individual species and the combined mosses, the SWIR indices, MSI and NDII, were more strongly correlated. However, although correlation is high, the model is weak, and a mixed model repeated measures approach was used to generate a more robust model. While some individuals displayed a decay function, the distribution on average was sigmoidal in nature, with the

best model for each index being the Gompertz model (asymmetric about the inflection point) which aligns with the theoretical distribution of the bounded indices I investigated.

Variation in index response existed within species replicates and among spectral indices, but in general all were best modeled using the Gompertz function based on AIC scores (comparisons across the row, for each model type). The AIC scores can't tell which index performed best between species, however, based on figure 4 & 5, it appears NDWI and NDII both modeled the index behavior as a function of moisture content the best for all three moss communities. MSI and NDII are useful because they can be extracted from multispectral broadband imagery, whereas Normalized Difference Water Index (NDWI) may not because multispectral platforms such as Landsat 8 do not have a band centered close to 1200nm ([83]). In these cases, MSI and NDII may be the best indices to investigate moss moisture content. WBI and MSI performed well at very high moisture contents but had heteroskedastic behavior at low moistures (Figure 4 & 5). To generalize for both *S. capillifolium* and *S. lenense*, NDWI values that are negative correspond with dry moss (<50% moisture content) and values which are positive corresponded with wet moss (>50% moisture) (Figure 4). Despite being poor at predicting the spectral index between ~ 0-20% and ~80-100%, the moss reflectance signature at those moisture brackets look very similar indicating that this observation can be useful for remote sensing because it can indicate whether moss are wet or dry at their surface, and sphagnum species in particular strongly shift spectral characteristics once they reach ~50- 60% moisture content, as in III.1 and observed by May et al (2018) [16]. All moisture indices were significant in predicting moisture content of the mixed pleurocarpous moss, but NDWI again performed best (Figure 5). The logistic model for

mixed pleurocarpous NDVI did not perform well because there was large variation and small changes relative to moisture content, but modeling it with a linear model did produce significant results which is in agreement based on previous studies [16] (results not shown).

For the mixed moss, all three species grouped together to generalize remotely-sensed moisture content of mosses, all indices performed reasonably well, but once more NDWI and NDII appear to perform best (Figure 5). Ultimately, my results demonstrated that moisture indices derived from the NIR region (IR-A: 750nm -1,400nm) were the most strongly associated with moisture content, particularly NDWI, across all groups.

III. 3 – Derivative Spectra for Identifying Region for Classification

Various methodological approaches for spectral differentiability have been developed including the use of derivative spectra (see I.7) [57]. Van Aardt (2000), demonstrated that first and second derivative spectra were valuable in the separability of pine, poplar, and oak trees, as well as separating species within those groups, using stepwise, canonical and normal discriminant analysis generating accuracies ranging from 62% to 100% [64]. My results demonstrate that enough differences between moss and vascular plant spectra exist and can be identified using derivative spectroscopy such that using a technique such as Spectral Angle Mapper, classification should be highly effective. The shift in REIP between mosses and vascular plants coupled with the increasing positive slope from the RE into the NIR for the moss samples (compared to a sharp RE and plateau for vascular plants) serve as crucial distinguishing characteristics. Though beyond the scope of this thesis, several techniques could be used to test how well

vascular and mosses can be separated, but here the objective was to determine which regions can be used for such approaches. The REIP for mosses from this study was similar to that of Bubier et al (1997) who used various different sphagnum and feather moss species (Sphagnum species ranged from 0.682-0.704nm and feather mosses from 0.682-0.684nm) [45]. Moss sample REIP was only slightly different among species and as samples dried (results not shown). Harris et al (2005), reported small shifts in REIP as mosses dried, but the REIP shift was typically less than 4nm which would be hard to detect with remote sensing platforms with broad bandwidths [48]. High resolution multispectral platforms like Sentinel-2 band 5, 6, 7 (central wavelength =704.1nm, 740.5nm, 782.8nm respectively with each band having bandwidth of 15nm, 15nm, and 20nm respectively) can likely detect these differences (moss slope positive from 680nm-~930nm), but hyperspectral platforms such as AVIRIS-NG which have hundreds of contiguous bands would be ideal. However, a satellite platform that lacks bands in the RE and NIR would not be able to pick up these subtleties, thus when trying to classify and study mosses from a satellite sensor platform, care must be taken in selecting the right sensor platform which can pick up the key regions in the RE and NIR. (Figure X).

III.4 – Rehydration Pilot Study

This pilot study was conducted to test whether reflectance changes in mosses as affected by moisture content drives plot-level reflectance. In these inter-tussock spaces and atop of hummocks, where moss species dominate the fine matrix of the understory and sometimes comprise the canopy, we determined that moss reflectance contributes to the overall signal significantly. Ecologically important indices such as NDVI at the moss-

level and to a slightly lesser extent at the community-level, were driven by short-term changes in moisture content. Though p-value of 0.08 for the community-level NDVI was only moderately significant, this result was likely due to small sample size. A power analysis was performed using the mean difference of NDVI and the standard deviation and the appropriate sample size to test for significance was determined to be 14.

MSI and NDWI were found to be highly correlated with moisture content from the drying experiment that was conducted earlier. Both these indices show that the moss and community-level moisture content could be remotely sensed and that community-level NDVI may be contingent on what the moisture status of the moss is since the vascular plants did not exhibit any significant change in response to short-term moisture fluctuations. Upon closer inspection, *S. capillifolium* and *S. lenense* community-level NDVI both increased significantly (NDVI diff = ~ 0.14 for each), but *S. angustifolium*, did not increase by as much (NDVI diff = ~ 0.02), possibly because of increased canopy cover. Mosses drove the community-level spectral signal. Hall et al. (1995) showed that sphagnum groundcover was an important component of remotely sensed imagery even in habitats dominated by large black spruce (*Picea mariana*) [67]. Spectral reflectance of arctic regions usually does not exhibit the typical plateau in the NIR common in vascular plants, likely because of low vegetation height and green leaf area where less backscattering of light occurs, and the understory (composed of mosses and lichens) reduces NIR reflectance [49, 68]. This phenomenon is exacerbated in the high arctic because of the smaller vegetation height and less abundant green vegetation compared with the low arctic.

Future studies should investigate the effects of canopy cover on mosses overall spectral contribution, but expectations would be that under high canopy cover, mosses will not have marked influence on overall spectra. However, under no, low or medium canopy cover, mosses are driving the spectral signal, most noticeable particularly when they are dry, and their relative reflectance is higher compared to vascular plants. Perhaps hyperspectral imagery at the beginning of the season prior to leaf-out can be used to gauge the understory inhabitants and their relative effects on those same pixels after leaf-out. With refined mixed models which incorporate endmember spectra of mosses, it may be possible to study the abundance and distribution of mosses and how they change over time. This could be accomplished with the use of repeated flight lines of hyperspectral sensors at low elevation like AVIRIS-NG or from multispectral daily satellite imagery from a platform like sentinel-2 or future platforms as resolution continues to improve. More experiments are needed to test whether this phenomenon scales up, nevertheless, satellite imagery is becoming so high resolution (Worldview-3: 30cm x 30cm panchromatic, 1.24m multispectral) that these small-scale plot level changes should eventually be detected. It is possible that even at the large-scale low-resolution platforms such as Landsat 8, this phenomenon may be observed when comparing signals before and after rain events.

V. Conclusion

Given the manner mosses can drive community-level spectra, particularly in the NIR/SWIR, large errors may be introduced into productivity models which rely on spectral indices such as NDVI. This study underpins the significance of understanding

the effects of moisture content in mosses on spectral reflectance when analyzing satellite or ariel imagery because of the drastic variation in the spectral profile under varying moisture content. Various moisture indices can be used to reliably predict moisture content, particularly those derived from the NIR (IR-A) such as NDWI, thus providing the remote-sensing specialist valuable information for interpreting their datasets. Conveniently, mosses and vascular plants have different spectral characteristics, particularly in the shape of the red edge and position of the REIP, which can be used to both classify and discriminate unknown spectra. In the sparse canopy of arctic vegetation, mixed pixels will generally contain vascular as well as non-vascular plants. The mixtures of moss patch sizes and heterogeneity combined with canopy cover make it challenging to separate them spectrally. Nevertheless, ever-increasing computational power, higher resolution imagery, and AI algorithm methodologies in derivative analysis techniques and spectral unmixing will improve precision in mapping vegetation to the species level and estimating ecosystem structure and function. Ultimately, it will be possible to estimate proportional presence of the endmembers in the mixed pixels [37]. This capability will aid in identifying abundances and distributions remotely at a crucial tipping point of arctic systems undergoing immense change.

Literature cited

1. Pielou, E.C., *A naturalist's guide to the Arctic*. 2012: University of Chicago Press.
2. Stow, D.A., et al., *Remote sensing of vegetation and land-cover change in Arctic Tundra Ecosystems*. *Remote sensing of environment*, 2004. **89**(3): p. 281-308.
3. Huemmrich, K., et al., *Remote sensing of tundra gross ecosystem productivity and light use efficiency under varying temperature and moisture conditions*. *Remote Sensing of Environment*, 2010. **114**(3): p. 481-489.
4. Hope, A. and D. Stow, *Shortwave reflectance properties of arctic tundra landscapes*, in *Landscape Function and Disturbance in Arctic Tundra*. 1996, Springer. p. 155-164.
5. Mogensen, G.S., *Illustrated Moss Flora of Arctic North America and Greenland: 3. Andreaeobryaceae-Tetraphidaceae*. Vol. 3. 1987: Museum Tusculanum Press.
6. Lovelock, C.E. and S.A. Robinson, *Surface reflectance properties of Antarctic moss and their relationship to plant species, pigment composition and photosynthetic function*. *Plant, Cell & Environment*, 2002. **25**(10): p. 1239-1250.
7. Green, T.A., et al., *UV-A protection in mosses growing in continental Antarctica*. *Polar biology*, 2005. **28**(11): p. 822-827.
8. Van Gaalen, K.E., L.B. Flanagan, and D.R. Peddle, *Photosynthesis, chlorophyll fluorescence and spectral reflectance in Sphagnum moss at varying water contents*. *Oecologia*, 2007. **153**(1): p. 19-28.
9. Wrona, F.J., et al., *Transitions in Arctic ecosystems: Ecological implications of a changing hydrological regime*. *Journal of Geophysical Research: Biogeosciences*, 2016. **121**(3): p. 650-674.
10. Chapin III, F.S., et al., *Arctic ecosystems in a changing climate: an ecophysiological perspective*. 2012: Academic Press.
11. Van Breemen, N., *How Sphagnum bogs down other plants*. *Trends in ecology & evolution*, 1995. **10**(7): p. 270-275.
12. Proctor, M.C. and Z. Tuba, *Poikilohydry and homoihydry: antithesis or spectrum of possibilities?* *New Phytologist*, 2002. **156**(3): p. 327-349.
13. Vogelmann, J.E. and D.M. Moss, *Spectral reflectance measurements in the genus Sphagnum*. *Remote Sensing of Environment*, 1993. **45**(3): p. 273-279.

14. Harris, A., *Spectral reflectance and photosynthetic properties of Sphagnum mosses exposed to progressive drought*. *Ecohydrology: Ecosystems, Land and Water Process Interactions, Ecohydrogeomorphology*, 2008. **1**(1): p. 35-42.
15. Van Gaalen, K.E., *Photosynthetic CO₂ exchange and spectral vegetation indices of boreal mosses*. 2005, Lethbridge, Alta.: University of Lethbridge, Faculty of Arts and Science, 2005.
16. May, J.L., et al., *Short term changes in moisture content drive strong changes in Normalized Difference Vegetation Index and gross primary productivity in four Arctic moss communities*. *Remote Sensing of Environment*, 2018. **212**: p. 114-120.
17. Gornall, J., et al., *Arctic mosses govern below-ground environment and ecosystem processes*. *Oecologia*, 2007. **153**(4): p. 931-941.
18. Olivas, P.C., et al., *Effects of fine-scale topography on CO₂ flux components of Alaskan coastal plain tundra: Response to contrasting growing seasons*. *Arctic, Antarctic, and Alpine Research*, 2011. **43**(2): p. 256-266.
19. Rautiainen, M., et al., *Coupling forest canopy and understory reflectance in the Arctic latitudes of Finland*. *Remote Sensing of Environment*, 2007. **110**(3): p. 332-343.
20. Suzuki, K., et al., *Moss beneath a leafless larch canopy: influence on water and energy balances in the southern mountainous taiga of eastern Siberia*. *Hydrological Processes: An International Journal*, 2007. **21**(15): p. 1982-1991.
21. Verbyla, D., *The greening and browning of Alaska based on 1982–2003 satellite data*. *Global Ecology and Biogeography*, 2008. **17**(4): p. 547-555.
22. Williams, M. and E.B. Rastetter, *Vegetation characteristics and primary productivity along an arctic transect: implications for scaling-up*. *Journal of Ecology*, 1999. **87**(5): p. 885-898.
23. Gamon, J., J. Penuelas, and C. Field, *A narrow-waveband spectral index that tracks diurnal changes in photosynthetic efficiency*. *Remote Sensing of environment*, 1992. **41**(1): p. 35-44.
24. Tucker, C.J., *A critical review of remote sensing and other methods for non-destructive estimation of standing crop biomass*. *Grass and Forage Science*, 1980. **35**(3): p. 177-182.
25. Rouse Jr, J.W., et al., *Monitoring vegetation systems in the Great Plains with ERTS*. 1974.

26. Filella, I. and J. Penuelas, *The red edge position and shape as indicators of plant chlorophyll content, biomass and hydric status*. International Journal of Remote Sensing, 1994. **15**(7): p. 1459-1470.
27. Eck, T., D. Deering, and L. Vierling, *Arctic tundra albedo and its estimation from spectral hemispheric reflectance*. International Journal of Remote Sensing, 1997. **18**(17): p. 3535-3549.
28. Zarco-Tejada, P.J., et al., *Vegetation stress detection through chlorophyll a+ b estimation and fluorescence effects on hyperspectral imagery*. Journal of environmental quality, 2002. **31**(5): p. 1433-1441.
29. Wulder, M.A., et al., *Surveying mountain pine beetle damage of forests: A review of remote sensing opportunities*. Forest Ecology and management, 2006. **221**(1-3): p. 27-41.
30. Wang, L. and J.J. Qu, *NMDI: A normalized multi-band drought index for monitoring soil and vegetation moisture with satellite remote sensing*. Geophysical Research Letters, 2007. **34**(20).
31. Westergaard-Nielsen, A., et al., *Camera derived vegetation greenness index as proxy for gross primary production in a low Arctic wetland area*. ISPRS Journal of Photogrammetry and Remote Sensing, 2013. **86**: p. 89-99.
32. Garrouste, E., A. Hansen, and R. Lawrence, *Using NDVI and EVI to map spatiotemporal variation in the biomass and quality of forage for migratory elk in the Greater Yellowstone Ecosystem*. Remote Sensing, 2016. **8**(5): p. 404.
33. Walker, D., et al., *Phytomass, LAI, and NDVI in northern Alaska: Relationships to summer warmth, soil pH, plant functional types, and extrapolation to the circumpolar Arctic*. Journal of Geophysical Research: Atmospheres, 2003. **108**(D2).
34. Morawitz, D.F., et al., *Using NDVI to assess vegetative land cover change in central Puget Sound*. Environmental monitoring and assessment, 2006. **114**(1-3): p. 85-106.
35. Yengoh, G.T., et al., *Use of the Normalized Difference Vegetation Index (NDVI) to Assess Land Degradation at Multiple Scales: Current Status, Future Trends, and Practical Considerations*. 2015: Springer.
36. Gu, Y., et al., *NDVI saturation adjustment: A new approach for improving cropland performance estimates in the Greater Platte River Basin, USA*. Ecological Indicators, 2013. **30**: p. 1-6.

37. Jensen, J.R., *Introductory Digital Image Processing: A Remote Sensing Perspective*. 2015: Prentice Hall Press.
38. Vourlitis, G.L., et al., *Physiological models for scaling plot measurements of CO₂ flux across an arctic tundra landscape*. *Ecological Applications*, 2000. **10**(1): p. 60-72.
39. Peñuelas, J., et al., *Estimation of plant water concentration by the reflectance water index WI (R900/R970)*. *International journal of remote sensing*, 1997. **18**(13): p. 2869-2875.
40. Hunt Jr, E.R. and B.N. Rock, *Detection of changes in leaf water content using near-and middle-infrared reflectances*. *Remote sensing of environment*, 1989. **30**(1): p. 43-54.
41. Gao, B.-C., *NDWI—A normalized difference water index for remote sensing of vegetation liquid water from space*. *Remote sensing of environment*, 1996. **58**(3): p. 257-266.
42. Hardisky, M., V. Klemas, and M. Smart, *The influence of soil salinity, growth form, and leaf moisture on the spectral radiance of Spartina alterniflora*, 1983. **49**: p. 77-83.
43. Shaw, A.J. and B. Goffinet, *Bryophyte biology*. 2000: Cambridge University Press.
44. Goffinet, B., *Bryophyte biology*. 2008: Cambridge University Press.
45. Bubier, J.L., B.N. Rock, and P.M. Crill, *Spectral reflectance measurements of boreal wetland and forest mosses*. *Journal of Geophysical Research: Atmospheres*, 1997. **102**(D24): p. 29483-29494.
46. Vogelmann, T.C., *Plant tissue optics*. *Annual review of plant biology*, 1993. **44**(1): p. 231-251.
47. Lee, D.W. *Plant tissue optics: micro-and nanostructures*. in *Biomimetics and Bioinspiration*. 2009. International Society for Optics and Photonics.
48. Harris, A., R. Bryant, and A. Baird, *Detecting near-surface moisture stress in Sphagnum spp.* *Remote Sensing of Environment*, 2005. **97**(3): p. 371-381.
49. Buchhorn, M., et al., *Ground-based hyperspectral characterization of Alaska tundra vegetation along environmental gradients*. *Remote Sensing*, 2013. **5**(8): p. 3971-4005.

50. Curran, P.J., *Remote sensing of foliar chemistry*. Remote sensing of environment, 1989. **30**(3): p. 271-278.
51. Main, R., et al., *An investigation into robust spectral indices for leaf chlorophyll estimation*. ISPRS Journal of Photogrammetry and Remote Sensing, 2011. **66**(6): p. 751-761.
52. BUTLER, W.t. and D. Hopkins, *Higher derivative analysis of complex absorption spectra*. Photochemistry and Photobiology, 1970. **12**(6): p. 439-450.
53. Demetriades-Shah, T.H., M.D. Steven, and J.A. Clark, *High resolution derivative spectra in remote sensing*. Remote Sensing of Environment, 1990. **33**(1): p. 55-64.
54. Fell, A.F. and G. Smith. *Higher derivative methods in ultraviolet-visible and infrared spectrophotometry*. in *Analytical Proceedings*. 1982.
55. Kim, R.S., *Spectral matching using bitmap indices of spectral derivatives for the analysis of hyperspectral imagery*. 2011, The Ohio State University.
56. Tsai, F. and W.D. Philpot, *A derivative-aided hyperspectral image analysis system for land-cover classification*. IEEE Transactions on Geoscience and Remote Sensing, 2002. **40**(2): p. 416-425.
57. Bahrami, M. and M.R. Mobasheri, *Plant species determination by coding leaf reflectance spectrum and its derivatives*. European Journal of Remote Sensing, 2020. **53**(1): p. 258-273.
58. Penuelas, J., et al., *Assessing community type, plant biomass, pigment composition, and photosynthetic efficiency of aquatic vegetation from spectral reflectance*. Remote Sensing of Environment, 1993. **46**(2): p. 110-118.
59. Philpot, W.D., *The derivative ratio algorithm: avoiding atmospheric effects in remote sensing*. IEEE Transactions on Geoscience and Remote Sensing, 1991. **29**(3): p. 350-357.
60. Walker, D.A., et al., *The circumpolar Arctic vegetation map*. Journal of Vegetation Science, 2005. **16**(3): p. 267-282.
61. Kelly Fretwell, B.S. *Sphagnum Capillifolium - small red peat moss*. 2021 [cited 2021 9/28/2021]; Available from: <https://www.centralcoastbiodiversity.org/small-red-peat-moss-bull-sphagnum-capillifolium.html>.

62. Walker, D. and M. Walker, *Terrain and vegetation of the Innavait Creek watershed*, in *Landscape Function and Disturbance in Arctic Tundra*. 1996, Springer. p. 73-108.
63. Lehnert, L.W., et al., *Hyperspectral Data Analysis in R: The hsdar Package*. Journal of Statistical Software, 2019. **89**(12): p. 1 - 23.
64. van Aardt, J.A., *Spectral separability among six southern tree species*. 2000, Virginia Tech.
65. Murray, K., J. Tenhunen, and R. Nowak, *Photoinhibition as a control on photosynthesis and production of Sphagnum mosses*. Oecologia, 1993. **96**(2): p. 200-207.
66. Harley, P., et al., *Irradiance and temperature effects on photosynthesis of tussock tundra Sphagnum mosses from the foothills of the Philip Smith Mountains, Alaska*. Oecologia, 1989. **79**(2): p. 251-259.
67. Hall, F.G., Y.E. Shimabukuro, and K.F. Huemmrich, *Remote sensing of forest biophysical structure using mixture decomposition and geometric reflectance models*. Ecological applications, 1995. **5**(4): p. 993-1013.
68. Liu, N., P. Budkewitsch, and P. Treitz, *Examining spectral reflectance features related to Arctic percent vegetation cover: Implications for hyperspectral remote sensing of Arctic tundra*. Remote sensing of environment, 2017. **192**: p. 58-72.
69. Taylor, P.C., et al., *Covariance between Arctic sea ice and clouds within atmospheric state regimes at the satellite footprint level*. Journal of Geophysical Research: Atmospheres, 2015. **120**(24): p. 12656-12678.
70. Schuur, E.A., et al., *Plant species composition and productivity following permafrost thaw and thermokarst in Alaskan tundra*. Ecosystems, 2007. **10**(2): p. 280-292.
71. Osterkamp, T., et al., *Physical and ecological changes associated with warming permafrost and thermokarst in interior Alaska*. Permafrost and Periglacial Processes, 2009. **20**(3): p. 235-256.
72. Olivas, P.C., et al., *Responses of CO₂ flux components of Alaskan Coastal Plain tundra to shifts in water table*. Journal of Geophysical Research: Biogeosciences, 2010. **115**(G4).
73. McGuire, A.D., et al., *Integrated regional changes in arctic climate feedbacks: implications for the global climate system*. Annu. Rev. Environ. Resour., 2006. **31**: p. 61-91.

74. Leffler, A.J. and J.M. Welker, *Long-term increases in snow pack elevate leaf N and photosynthesis in Salix arctica: responses to a snow fence experiment in the High Arctic of NW Greenland*. Environmental Research Letters, 2013. **8**(2): p. 025023.
75. Post, E., et al., *Ecological dynamics across the Arctic associated with recent climate change*. science, 2009. **325**(5946): p. 1355-1358.
76. Reynolds, J., et al., *Patch and landscape models of Arctic Tundra: potentials and limitations*, in *Landscape function and disturbance in arctic tundra*. 1996, Springer. p. 293-324.
77. Kattsov, V.M., et al., *Simulation and projection of Arctic freshwater budget components by the IPCC AR4 global climate models*. Journal of Hydrometeorology, 2007. **8**(3): p. 571-589.
78. Dickson, R., et al., *The Arctic ocean response to the North Atlantic oscillation*. Journal of Climate, 2000. **13**(15): p. 2671-2696.
79. Hare, S.R. and N.J. Mantua, *Empirical evidence for North Pacific regime shifts in 1977 and 1989*. Progress in oceanography, 2000. **47**(2-4): p. 103-145.
80. Roulet, N., et al., *Northern fens: methane flux and climatic change*. Tellus B, 1992. **44**(2): p. 100-105.
81. Houghton, J.T., G.J. Jenkins, and J.J. Ephraums, *Climate change*. 1991.
82. Kobayashi, H., et al., *Spectral reflectance and associated photograph of boreal forest understory formation in interior Alaska*. Polar Data J, 2018. **2**: p. 14-29.
83. Barsi, J.A., et al., *The spectral response of the Landsat-8 operational land imager*. Remote Sensing, 2014. **6**(10): p. 10232-10251.